EXPERT REBUTTAL REPORT

DEEPWATER HORIZON BLOWOUT PREVENTER EXAMINATION AND TESTING

November 7, 2011

Prepared by:
The team of Talas Engineering, Inc.
20902 Cabot Blvd.
Hayward, CA 94545

Lead Author
Dr. Rory R. Davis, PE

Contributing Authors
Patrick R. Novak, PE
J. Neil Robinson, PhD
Raymond Merala, MS, PE

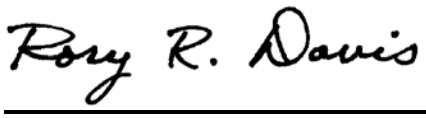

Rory R. Davis, PhD, PE

s/ J. Neil Robinson, PhD
J. Neil Robinson, PhD

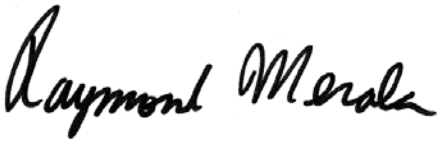

s/ Patrick Novak
Patrick R. Novak, PE

Raymond Merala, MS, PE

TREX-07661

TABLE OF CONTENTS

I. INTRODUCTION

An original report was submitted on August 26, 2011, and following is a rebuttal report, responding to comments and analysis offered by other experts in this matter. See the previous report for our expert qualifications and prior testimony. Attachments 4 through 7 provide recent updates to legal testimony by our experts.

The reader of this report is assumed to already be knowledgeable about the Deepwater Horizon events, to have some knowledge of the Blowout Preventer (BOP) systems, and have reviewed recent expert reports pertaining to the Deepwater Horizon incident, especially the reports of Greg Childs, Arthur Zatarain, Forrest Earl Shanks II, Cliff Knight, and David L. O'Donnell pertaining to the BOP aspects.

As with our first report, our opinions focus on aspects of the BOP, including the Lower Marine Riser Package (LMRP), the lower BOP stack, and their constituent parts, associated controls, drill pipe, riser, and related ROV activities.

Opinions with sufficient data/information to be of reasonable engineering and logical certainty are given following. We reserve the opportunity to provide additional opinions, or augment current opinions at a later date, or respond to further opinions from other experts, if more information becomes available.

Specific citations used to support the basis of opinions are provided in section IV, References Cited, and are referenced in brackets [ ]. Attachment 8 is a complete listing of documents considered in preparing this report.

II. EXECUTIVE SUMMARY

We have revewed several expert reports, including those mentioned above, regarding operation of the BOP on the Deepwater Horizon. In response to the opinions and analysis presented in these reports, we have perfomed additional analysis which, as explained below, confirms the opinions offered in our original report. Furthermore, the analyses illuminated more details concerning the incident. Opinions are summarized below, and details will be discussed later, including reference sources.

1. Upward forces in the well would not have been sufficient to cause the drill pipe to be pushed off-center at the time the AMF could have functioned. Upward force calculations relied on by other experts to explain the drill pipe being off-center are incorrect. This conclusion applies both to claimed forces from well hydrostatic pressure and from well flow.

2. The starboard side ram on the Upper Variable Bore Ram (UVBR) was not locked at the time of the incident nor at any time before the blind shear ram (BSR) was activated by the Autoshear. Evidence shows this ram was able to and did move.

3. The BSR did not activate at the time of AMF. Contrary to the opinions provided by other experts, the drill pipe was sufficiently centered at the time of AMF, and the BSR would then have been capable of sealing the well. Detailed analysis of the sequence of events demonstrates that the BSR was first activated at the time the Autoshear pin was cut on the morning of April 22, 2010. The BSR then failed to seal the well because the drill pipe was off-center at this time.

4. The opinion offered by Cliff Knight, on behalf of Cameron, that the drill pipe was centered at the time of BSR shear is unfounded.

5. The opinion offered by both Cliff Knight and David L. O'Donnell, on behalf of Cameron, that the BSR would not have been able to seal the well even if the pipe had been centered is unsubstantiated.

6. The Deepwater Horizon BSR had poor ability to center pipe, especially in comparison to other designs.

7. The miswired 103Y solenoid was positively faulty and prevented AMF operation from the Yellow pod.

8. The Blue pod 27V battery was positively depleted and prevented AMF operation from the Blue pod.

III. STATEMENT OF OPINIONS

3.1. UPWARD FORCES IN THE WELL WOULD NOT HAVE BEEN SUFFICIENT TO CAUSE THE DRILL PIPE TO BE PUSHED OFF-CENTER AT THE TIME THE AMF COULD HAVE FUNCTIONED

Mr. Childs, whose testimony is offered by Transocean, contends that helical buckling in the drill pipe was caused by wellbore pressure and dynamic flow causing the drill pipe to be off-center at the time of AMF activation. [Ref. 2 p. 2] A complete explanation has not been provided of upward force prediction assumptions and methodology with annulus or drill pipe flow, or without flow. It is counter-intuitive that such upward forces could be so large as to cause buckling, especially for the no-flow hydrostatic conditions. Therefore, in response to this contention, an analysis was performed using first principles, and is described below. All assumptions and methodologies are contained in Attachment 1.

In addition, we have identified an error in the flow and associated flow force calculations by Stress Engineering Services (SES) [Ref. 1], relied upon by Mr. Childs, that hugely over-predicts flow velocities and forces below the BOP [Ref. 2, Figure 15].

SES gives a hydrocarbon (HC) gas-only expansion analysis (starting on page 126) to predict flow rate for fluids being pushed out at the rig by the HC gas expansion, and reports (p. 128) volumetric flow rates at the rig in the several 100's of ft/sec near explosion time. [Ref. 1] However, volumetric flow rates below the BOP down to the bottom of the drill string would be much less than the volumetric flow rates at the rig, due to the HC not having expanded to a gas yet. At those depths the HC is still a supercritical fluid under substantial pressure, which is much denser than a gas and is much more compressible than fluid because it contains gas in solution. Nevertheless, SES appears to incorrectly use the very same volumetric flow rate data from gas-only analysis to calculate the behavior of the supercritical fluid in the annulus. [Ref. 1, pp. 132-133] These same calculations are further used to incorrectly calculate the axial forces that were then relied upon by Mr. Childs to reach his conclusion that the drill pipe was off-center at the time of AMF [Ref. 1, pp. 141-142, Ref. 2, Figure 15].

In apparent contradiction to the above described analysis, SES later decribes a "Scenario 2" calculation of the flow rate, for the time just prior to VBR closure, and finds an average volumetric flow rate at a 5-1/2" pipe tool joint in the casing of 120 ft/sec. [Ref. 1, p. 144] The majority of upward flow force is not produced at tool joints; the vast majority of pipe length is smaller diameter, and the flow rate there would be much less, and that lower value is appropriate for force calculations. One can calculate that lower value at nominal pipe annulus by simple area ratio versus the tool joint annulus. The "average" flow rate at nominal pipe walls per SES Scenario 2 would be 68.9 ft/sec, much lower than the huge flow rates assumed by Childs. [Ref. 1, p. 142] It appears that Childs ignored Scenario 2, but this flow rate magnitude seems more reasonable in our opinion. SES did not calculate pipe forces for Scenario 2.

Further, the HC is supercritical, and as such should be analyzed on a more piecewise or vertical-position dependent basis, to account for large changes in density as it flows upward. SES noted that in fact the properties are highly variable, providing HC properties as a function of pressure. [Ref. 1, p. 132]

To respond to the analysis proffered by Mr. Childs, as described below and in more detail in Attachment 1, we have done calculations of the forces on the drill pipe using some of the assumptions provided by SES. The flow and forces are analyzed by conventional methods accounting for vertical variation of fluid properties, pipe size changes, and annulus OD changes.

CASE A

The first calculation, denoted CASE A, is done for the time just before VBR closure and the explosion. Assumptions of the analysis are made for "apples and apples" comparison to SES's "Scenario 2" (22,299 lbm/day mass flow rate in annulus) and uses SES HC density and viscosity data as a function of pressure. [Ref. 1, p. 144]

This analysis gives a resulting upward compression in the drill pipe walls at the VBR of 21.6 kip at this time. Using SES's own blowout flow assumption, the forces are far less than the assumed 30-150 kip by SES in *Structural Analysis of the Macondo #252 Work String* [Ref. 3], and notably far less than any drill pipe Euler buckling force limit of more than 100 kip [Ref. 3 & 4].

Figure 1 shows the new drill pipe wall force variation with depth. Note that step force changes at pipe size changes are clear, and known to be present, but were not apparent in the SES work, for example Fig 3 of Reference 3. This is a clear indicator of incorrect analysis by SES.

CASE B

The next case, CASE B, is considered for forces immediately after the VBR was closed. The analysis methodology is the same as for the flow case above, except to set the flow to a negligible level, and the flow delta p and pipe surface tractions go away, leaving the hydrostatic result immediately after flow stops. The closed drill pipe pressure at the rig is the same as before at this time, but only momentarily.

The CASE B analysis gives a resulting downward tension in the drill pipe walls at the VBR of 36.5 kip at this time. The forces are in the opposite direction than the assumed 30-150 kip compression by SES, and substantially so. [Ref. 3]

Figure 2 shows the new drill pipe wall force variation with depth for CASE B. Note that step force changes at pipe size changes are again clear, and known to be present. In fact the force step at the pipe transition above the BOP is reversed from the previous case.

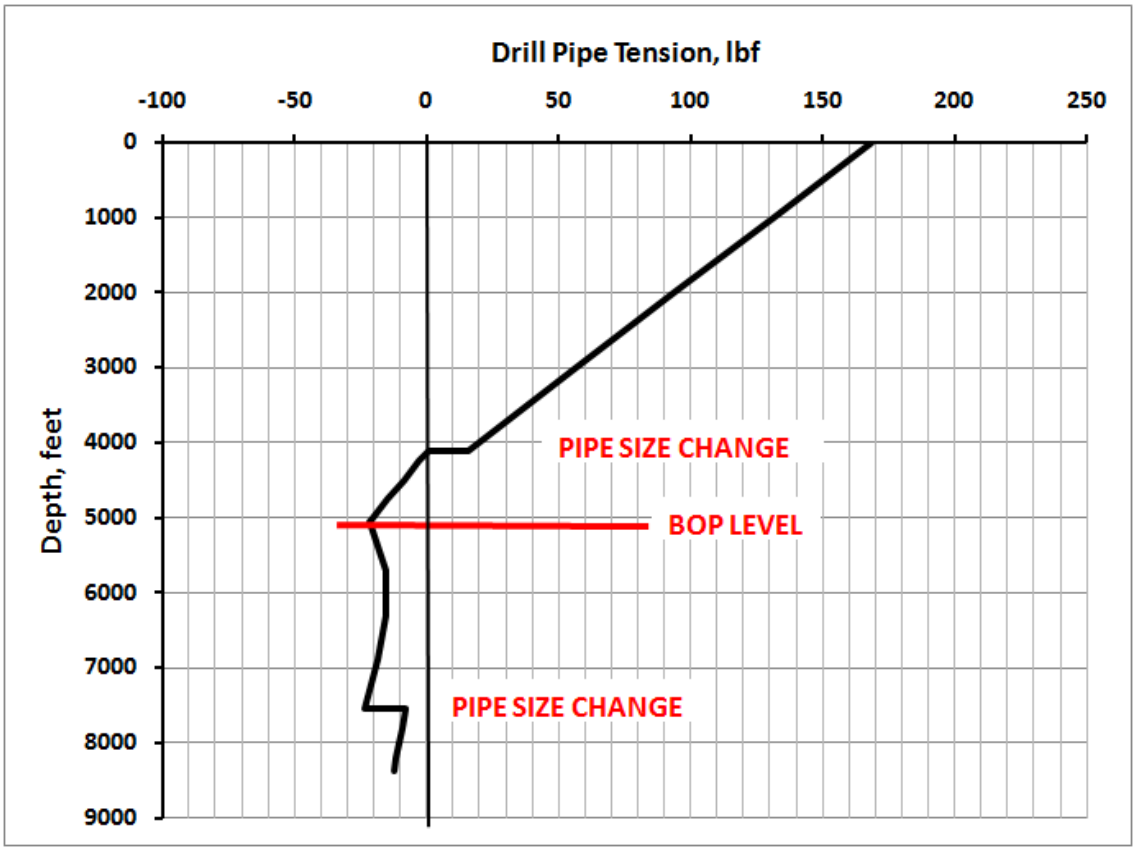

Figure 1. Pipe wall tension forces for CASE A, annulus flow just before VBR closure

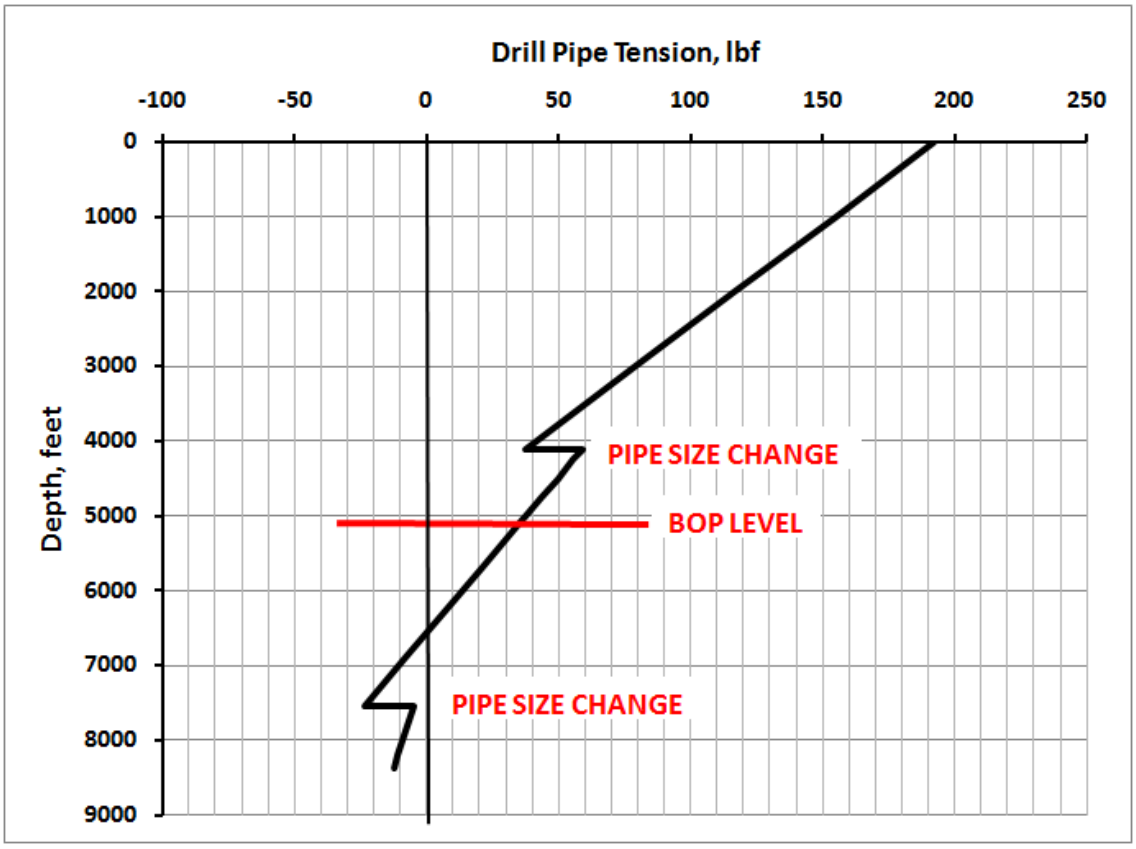

Figure 2. Pipe wall tension forces for CASE B, no annulus flow just after VBR closure

This condition of CASE B is momentary. Given some time, the HC in the annulus above the closed VBR will flash to gas and expand, and fluids above that gas will continue to flow upward due to that gas expansion onto the rig, and pressure in the annulus will decrease. At the same time, pressure in the drill pipe and annulus below the closed VBR will increase due to the stoppage of flow from the formation and pressure buildup. Timing is not certain for this change.

CASE C

The last case, CASE C, thus assumes we have development of much higher pressure below the drill string, and substantial evacuation of the annulus above the VBR. This case is analyzed by SES (called the "VBR load case"), and relied upon by Mr. Childs as the no-flow condition that purportedly compresses the pipe into a helix. We use SES's assumption of 8,500 psi below the VBR and about 500 psi above it. [Ref. 3, p. 29] As the HC pressures are much higher now, we for an apples and apples comparison, assume the same HC densities as SES uses, constant 5 ppg below the VBR and 2 ppg above it. [Ref. 3, pp. 11, 29] For now, we also assume as SES does that the VBR can hold no axial force.

The CASE C analysis gives a resulting downward tension in the drill pipe walls at the VBR of 10.5 kip. The forces are in the opposite direction than the assumed 30-150 kip compression by SES. [Ref. 3 Figure 8]

Figure 3 shows the CASE C drill pipe wall force variation with depth. Note that step changes at pipe size changes are clear, and known to be present, but were not apparent in the SES work. The huge step in force at the closed VBR (and the VBR assumed to not hold axial force for this analysis for consistency with SES assumption) assumed by SES is erroneous and does not exist.

Conclusions About Loading

Looking at these results, it is clear that forces from below are much lower than Childs and SES contend, and the pipe undergoes a strong load reversal from compression to tension as the VBR closes. Also note that as the VBR nears closure, the flow forces would decrease and any compression pipe load would relax as the VBR comes closed. Compression transitions to tension before the VBR stops the flow. This virtually guarantees that if the rig was still station-keeping (and it was at this time, the explosion had not stopped power yet), the pipe would have been pulled and straightened even if it was bent some small amount by the lower forces of annulus flow before closure, and would be centered by the closure of a VBR.

Next, we consider that a closed VBR can carry some axial force. Despite SES's arguments, relied upon by Childs, VBRs can carry large amounts of vertical load when closed on pipe. [Ref. 3, 2] We have reviewed the analysis of vertical load carried by a closed VBR given by Earl Shanks in Appendix C to his report, whose testimony is offered by BP, and agree with his conclusion that frictional forces from the closed VBRs would be more than adequate to react substantial forces against pipe movement. [Ref. 5] While friction coefficients are difficult to know, and actual compression forces of packers against the pipe at closure can be influenced by wear and age of the packers, even if Shanks' analysis used substantially lower friction coefficients and clamping forces, the axial forces capable for a VBR to hold would still be quite large, and certainly enough to counter some movement of the drill pipe, either from forces from below or above.

After the VBR closed, the momentary 36.5 kip tension in the pipe at the VBR could have been "captured" at least partially, i.e. any later reduction in tension from below would not have transmitted directly to the

pipe above the VBR. Thus, at a later time, the tension in the pipe in the BOP could be between the 36.5 kip of CASE A and the 10.5 kip of CASE B. In any event, one would not expect the pipe to go into compression for some time, when the VBR(s) later loosen and start to leak, or when flow later ensues through the drill pipe because of some breach of the pipe above. Also note given that the BSR closes when Autoshear is activated, any accumulated looseness of the Middle VBR, if not too large, would be tightened up after the BSR closure, because then the ST locks would close and push the VBR closed again, although not with full force. Thus the fact that the VBR was loose could be disguised.

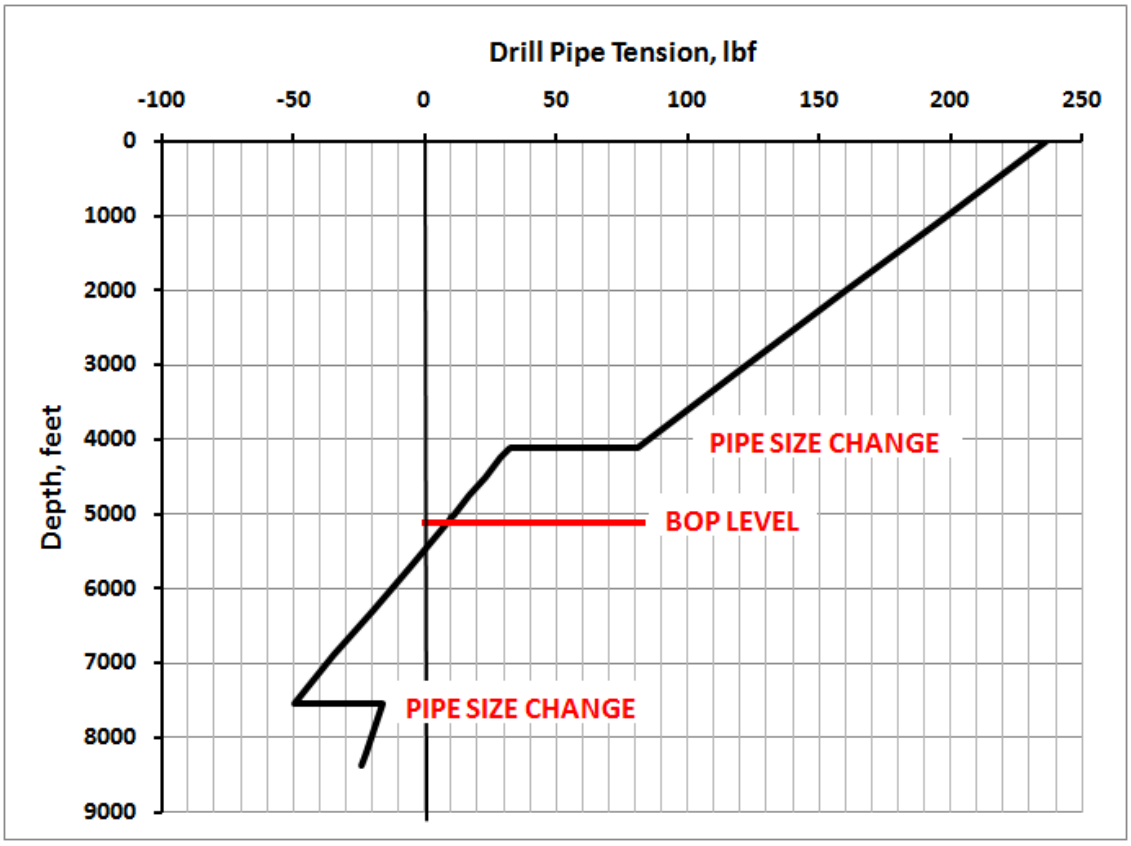

Figure 3. Pipe wall tension forces for CASE C, no annulus flow a while after VBR closure

These improved load analyses clearly show that forces of flow conditions or no-flow hydrostatic pressure conditions, from the time just before VBR closure to AMF time, are much less than SESs incorrect calculations showed, and Mr. Childs relied upon. Further, it is found that the drill pipe is pulled in tension, not heavily compressed, at the time of AMF. Finally a VBR if fully closed will center the pipe and is likely to hold substantial forces if the drill pipe attempts to move axially.

We also maintain that large force of pipe restraint by the UA , as claimed by Childs, is not substantiated. No analysis at all has been presented that the UA would have been capable of such restraint, and there are strong reasons to believe that it would not. First, after the explosion, the pressure had been lost from the UA, which would have allowed the packer to loosen around the pipe. Also, initial close pressure was apparently not maximum according to O'Donnell. [Ref. 16, Exhibit C] It is much more likely that any axial pipe restraint came from VBRs and/or the rig itself. The VBR load-carrying would mitigate the effect of any upward force effects from below, leaving pipe offset from effects above, such as rig drift, the remaining source.

Drill Pipe FEA With The Correct Loads

Given the aforementioned loads, drill pipe Finite Element Analysis (FEA) was performed to show reasonably expected pipe deflections under several conditions. The analysis is given in Attachment 1.

The model demonstates that at the time of AMF, after the Middle VBR has closed, under any reasonable axial load and up to 300 feet rig drift, the drill pipe would remain sufficiently centered to be cut by the BSR (Case 1 in Attachment 1). In contrast, as Case 3 outlined in Attachment 1 demonstrates, at a maximum flex joint tilt of 15 degrees, which would occur with about 1300 feet of rig drift or drift/current equivalent or more,[1] drill pipe will be substantially offset at the BSR, and just above the BSR the drill pipe contacts the well bore for a long distance. In addition, if one assumed that the UA holds vertically instead of the VBR, for the same pipe force, the BSR offset is about the same. Furthermore, the model demonstrates the obvious and entirely forseeable conclusion that movement and tilt of the flex joint, which it is designed to do in subsea operations, will result in offset position of the drill pipe in the wellbore.

3.2. THE STARBOARD SIDE UPPER VBR RAM WAS NOT LOCKED

Two reports submitted by other experts in this matter present arguments to rebut the opinion offered in our original report regarding how the drill pipe came to be positioned off-center. Mr. Shanks argues that our opinion that rig drift pushed the pipe off-center does not take into account the centering effect of the closed UVBR seven feet below the BSR. [Ref. 6, pg. 44] Mr. Childs claims that all the ST locks on the UVBR and MVBR being closed is proof that the AMF operated. [Ref. 2, pp. 13, 30] But ST locks can be closed by either AMF or Autoshear.[2] If the ST locks were not locked until Autoshear, then Mr. Childs apparently agrees that the rams would have been able to move open during the 33.5 hours until the autoshear pin was cut. That the rams did not so open, according to his claim, he takes as evidence of AMF operation. In view of these arguments, it is appropriate to examine what the evidence actually shows about the VBR rams and locks. As explained below, the starboard side ram on the UVBR was not locked at the time of the incident or any time before Autoshear. Evidence shows the starboard side ram of the UVBR could and did move, thus it could not restrain the the drill pipe at later times well after the AMF time.

There is general agreement that the rig crew closed the upper and middle variable bore rams just prior to loss of communication between the rig and the BOP, thus sealing off flow through the annulus for a period of time. Some time after the incident, in May 2010, the position of the locks was investigated radiographically. [Ref. 7] This investigation showed that both locks on the MVBR and on one side of the UVBR were closed. However, the position of the East (starboard) side UVBR lock could not be determined. [Ref. 7] Thus it appears the MVBR was fully closed and locked at some time before, but full closure and locking of the UVBR is not supported by the evidence. It is plausible that loss of hydraulics at the time of the explosion may have interfered with full closing of the UVBR, but that is uncertain.

In addition, it is helpful to consider the condition of the UVBR wear pads. Two wear pads are located underneath each ram block of the upper and middle VBRs, one on either side. The portion of the wear

[1] Rig drift of as much as 1600 feet was established in our first report

[2] ST locks are plumbed to close any time the main BSR valve is shifted via AMF or Autoshear function, therefore if they were closed this does not prove the AMF fired the BSR.

pad most exposed to the hot hydrocarbon on each wear pad swelled, softened in the heat, and discolored. See, for example, Figure 4.[3] When the wear pads cooled they became hard again, but the swelling, distortion and discoloring are still evident. Examination of the evidence shows that the appearance of the wear pads on the two UVBR rams is quite different. The wear pads on the starboard side (see Figures 4 and 5) show the wear pad material stretched and distorted, rather like pulling on taffy. Such distortion could only occur when the pad material was soft and therefore hot. This means that the ram moved while it was hot, ie. during the period of hydrocarbon flow. That the ram moved means in turn that this ram cannot have been locked.

The appearance of the wear pads on the port side UVBR is quite different, see Figures 6 and 7. The top of the swelled portion on each one is scraped flat. Such scratching and abrasion damage could only occur when the material was hard, as it would be when relatively cold. This damage therefore occurred after the period of hydrocarbon flow, apparently when the rams were opened after retrieval of the BOP. It is consistent with this ram having been locked. The wear pads on the MVBR rams are similar to those on the port UVBR, see Figure 8, consistent with both sides of the MVBR having been locked, and again differ from the starboard UVBR wear pads.

Further supporting evidence is provided by the erosion patterns on the drill pipe at the UVBR. These are distinctly asymmetric, indicating the two rams were closed to differing extents (see Figure 9). Note that the position of the locks as later measured at NASA Michoud is not indicative of their position at the time of the incident, because they had been cycled more than once between the time of the incident and inspection in New Orleans (see, for example Reference 8).

***Figure 4. Starboard UVBR. Note the brown, distorted area on the wear pad in the foreground. (*DNV IMG8297, December 16, 2010)**

[3] This analysis is based on first hand viewing of the parts, the photos are not as clear as first hand review.

Figure 5. Starboard UVBR. Wear pad is on the left. **(DNV IMG8294, December 16, 2010)**

Thus the evidence clearly establishes that the starboard side UVBR could and did move. With one ram able to move, the UVBR could not restrain and center the drill pipe. Furthermore, contrary to Childs' apparent argument that all rams being locked proved that the AMF operated, this ram was not locked and was able to move. It is also known that if ST locks are observed locked at some later date, they were not necessarily locked before Autoshear activation.

Figure 6. Port UVBR **(DNV IMG 8574, April 30, 2011)**

***Figure 7. Port UVBR. (*DNV IMG 2106, December 14, 2010)**

***Figure 8. Port MVBR. (*DNV IMG 8508, April 29, 2011)**

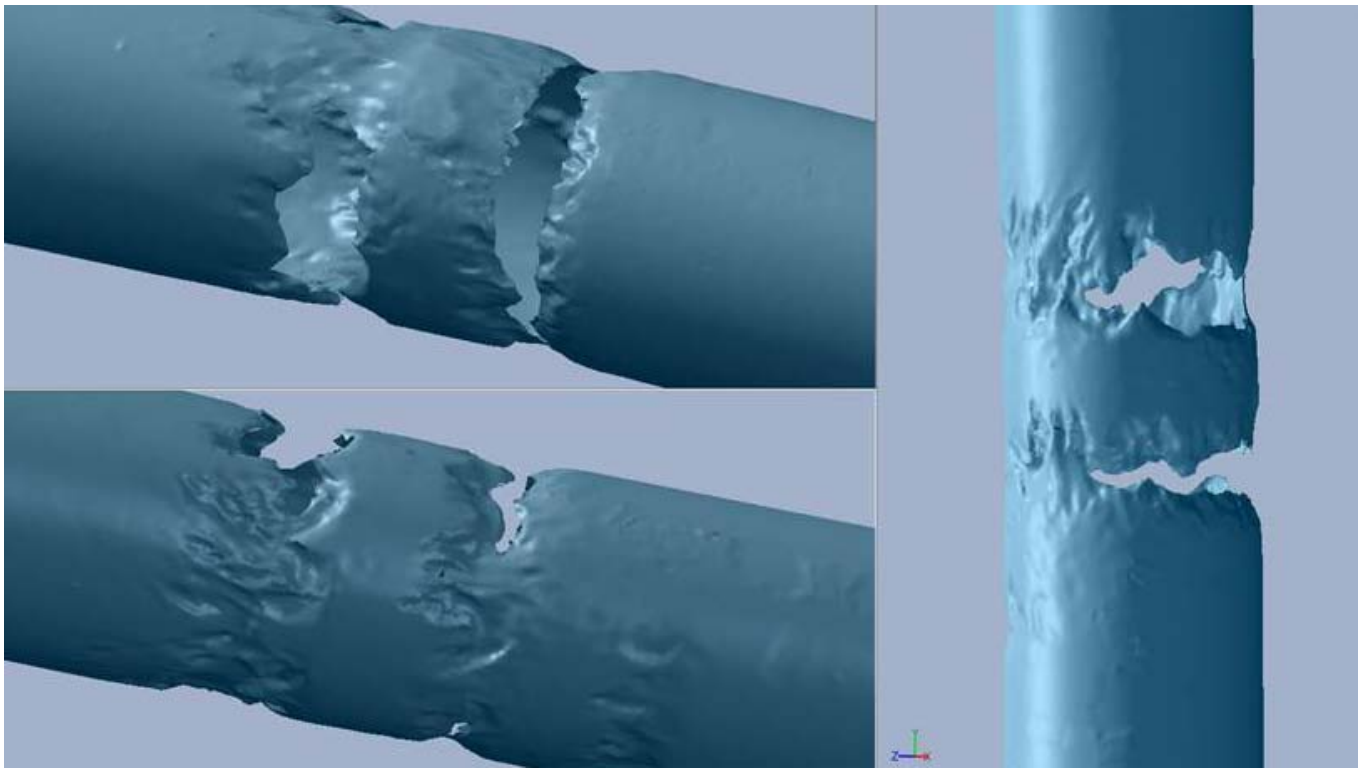

Figure 9. Erosion on the drill pipe at the UVBR (from page 82 of Reference 4)

3.3. THE BSR ACTIVATED BY AUTOSHEAR, NOT AMF, AND FAILED TO SEAL

The absence of large upward forces on the pipe, lack of Euler buckling, the rig still stationkeeping, the pipe being pulled straight by a large tension "tug" during a VBR closing, and a VBR centering the pipe in the wellbore all point to the virtually certain scenario that the pipe was centered in the BSR when the AMF could have fired very near explosion time. The observed fact that the pipe was offset in the BSR and the BSR not fully sealed clearly indicates BSR closure at a different time than AMF, which would be at Autoshear time much later.

Based on our analysis, we conclude the following facts are supported by the evidence, with some details to be further discussed in later sections and below.

1. The Upper Annular (UA) was closed around 21:42 April 20, 2010, but never did seal the well. [Ref. 1, p. 111-12, 146; Ref. 9 at Appendix I p. 90; Ref. 19 at pp. 28, 44] If it had, pressure increase would have been seen on the kill line, and both that pressure and the wellhead pressure would have increased greatly.

2. At least one VBR (for the reasons discussed in 3.2 probably the MVBR) was fully closed at 21:47 April 20, 2010 and did temporarily seal the well annulus (shut in the well). [Ref. 1, pg. 111-112; Ref. 19 at p. 44] The drill pipe was also known to be closed at that time at the rig (wellhead pressure was measured), so there was no HC flow from below. But by that time, enough HCs had risen above the BOP to cause the blowout and explosion at the rig by gas expansion in the riser.

3. Shortly after closure of the VBR, the explosion took place, severed BOP communications, and provided the conditions for the AMF to be triggered. [Ref. 1 at p. 112; Ref. 19 at pp. 44, 103] A VBR, probably the MVBR, had centered the pipe, and hydrostatic pressures had tensioned the pipe during VBR closure (as explained in 3.1). The UA was also centering the pipe from earlier closure.

4. At this time, the drill pipe was nearly centered, despite initial rig drift, and the drill pipe was in substantial tension (see 3.1 and pipe FEA in Attachment 1). The BSR was also not subjected to flow erosion at this time or before, nor extreme wellbore pressures, because the closed VBR blocked the annulus flow and the BSR had been retracted (open). The VBR was able to hold substantial axial force on the pipe at this time as well.

5. The BSR had good conditions to sever the drill pipe at this time, before the VBRs loosened up after loss of hydraulics in the explosion. Pressure from below would help keep the VBR closed for a short time by the "pressure assist" effect, [Ref. 20], there were no substantial side loads on the pipe that might wrench the VBR open (see pipe FEA in Attachment 1), and axial loads were not very large and were decreasing (due to boil-off of HC gas above the VBR).

6. After AMF triggering, the AMF sequence did not actuate the BSR (due to a dead 27V battery in the Blue Pod and the miswired 103Y solenoid in the Yellow pod). ST locks, which are also activated by the AMF via the same hydraulic plumbing as the BSR via Solenoid 103, consequently did not close either.[4]

7. At the time the AMF was triggered, the drill pipe was centered. Pressures above the VBR were low, and erosion of the BSR at this time was non-existent. Had the BSR closed at this time, it is almost certain it would have cut the pipe and sealed the well.

8. After the time at which the AMF was triggered, the rig drifted for many hours, bending the drill pipe laterally within the well bore via shifting the LMRP top flex joint (in lateral rotation), and pulling and pushing the drill pipe from the rig with substantial forces as the result of drift and sea currents. This movement loosened and partially opened at least the UVBR (or it had never completely closed at explosion time), and caused leaking at the VBRs after a time.

9. The loosening of the VBRs allowed greater lateral movement of the drill pipe within the BOP, in response to rig drift, sea current, and drill pipe tension/compression from the rig above. Upward flow forces developed from leakage of the VBRs were not large, nor were pA net upward forces very large.

10. At the time of Autoshear on April 22, 2010, the pipe was offset in the wellbore due to the relative freedom of the open UVBR, and accumulated movement of the drill pipe for many hours in the presence of some restraint from the MVBR. The Autoshear did actuate the BSR and ST locks (a hydraulic-only system). The BSR did not cut the drill pipe completely due to offset pipe, leaving the BSR partially open. However, based on the observations of distinct crush marks on the drill pipe from a corner of the BSR jaws, the pressure available to the BSR was clearly sufficient to cut the pipe had it been centered.

[4] It is unlikely that the rig crew activated the ST locks as this was not normal practice. [Ref. 1, Vol. 1 at 157; Ref. 21].

11. BSR exhaust flow at Autoshear time was not observed, because the field of view of the ROV video recording could not have seen it.

12. Shortly thereafter, at the time the Casing Shear Ram (CSR) was activated on April 29, 2010, the drill pipe was now relatively free below the BSR. [Ref. 7] The CSR uses steeply angled blades that can easily center the pipe, even against substantial forces. Thus, the CSR centered and cut the pipe. The lower pipe did not fall to the bottom of the well, indicating that the MVBR was still sufficiently closed to hold the pipe.

13. Some time after the BSR cut, pipe pieces above the BSR migrated upward (from drill pipe tension and/or flow force), and the rig sank and severely bent the riser a short time later on April 22, 2010. [Ref. 7]

14. Once the pipe was completely opened at the CSR after the cut, larger flows ensued at the CSR level, and continued to wash the CSR, BSR and Upper Annular for about 76 days. The UVBR and MVBR were washed by lesser annulus flow, less severely, as they were below the CSR and did not get the open pipe flow, and the Test Ram was not significantly washed because it had never been closed.[5]

While the above analysis is not changed from the opinions offered in our original report, the analysis has been refined in response to criticisms from the other reports as described.

3.4. THE ATTEMPT IN THE KNIGHT REPORT TO DEMONSTRATE THAT THE DRILL PIPE WAS CENTERED AT THE TIME OF BSR SHEAR IS UNFOUNDED

Cliff Knight, whose testimony is offered by Cameron, attempts to throw doubt on the drill pipe being off-center at the time of cut, by attempting to use the DNV laser scan models to match up the indentation on the pipe with it being centered on an eroded BSR blade, and thus not off-center when sheared. [Ref. 15] Mr Knight is the only expert to arrive at such an opinion.

There is clear physical evidence that the drill pipe was off-center at the time of the BSR shearing. Whether or not the theories as to why it was off-center are correct does not affect that it was off-center. The distinct press marks on the drill pipe are conclusive indicators of heavy contact with the outer lateral shapes of the BSR ram blocks, but not the only indicators. Nothing in the report offered by Mr. Knight compels a different conclusion.

In his report, Mr. Knight relies on documents and analysis of DNV laser scans. [Ref 15, p. 1). There is no indication in the report that Knight ever physically saw the evidence himself (drill pipe and rams), or engaged in a detailed examination. Mr. Knight also states that "all three reports rely on DNV's analysis of indentation marks". [Ref. 15, pg. 12] If this statement includes the report by Talas Engineering, this conclusion is incorrect. As stated in our prior report, our investigation and analysis included "information gathered and witnessed at the Michoud investigation," i.e., <u>first</u> hand information. Our report makes use of figures and photographs from DNV only because we were not allowed to take our own photographs or do our own scans. Our conclusion was not based on that of DNV, but rather, Talas Engineering concluded from <u>first</u> hand examination that there was clear evidence that the pipe was off-center when cut.

[5] Based on first-hand observations at Michoud.

3.5. THE CONTENTION IN THE KNIGHT AND O'DONNELL REPORTS THAT THE BSR WOULD NOT HAVE BEEN ABLE TO SEAL EVEN IF THE PIPE HAD BEEN CENTERED IS UNSUBSTANTIATED

According to Knight and O'Donnell, even if the BSR had activated at the time of AMF, and even with the pipe centered, the BOP would not have sealed the well, because flow from the cut drill pipe would have eroded the packers. [Ref. 15, pp. 6-7 & Ref 16, pp. 25-26] Therefore, they conclude, it would not matter whether or not the AMF operated. These statements are unsubstantiated. They are not backed up by analysis of the effect of flow on the packers or by consideration of how much reduction in flow there would have been if the BSR had closed completely, even if it had not fully sealed.[6] What is clear is that the opportunity to bring the blowout under control and reduce the adverse consequences would necessarily have been greater if the BSR had closed early (i.e., at AMF) than if (as actually happened) it never properly closed at all.

The pressure differential across the drill pipe was a maximum of about 7,400 psi at the time the AMF would have been triggered, according to Attachment 1 CASE C. This is not an unexpected operating pressure differential for drill pipe. This size and grade pipe can carry 12,780 psi differential (the pipe wall was also in tension at the time). Neither Knight nor O'Donnell explain clearly how cutting a pipe with such a pressure would actually wear away the seals of the BSR. Knight and O'Donnell's opinions in this respect are only conjecture until erosion rates for the condition in question can be quantified.

O'Donnell asserts that:

> Due to Extreme Well Conditions, the Blind Shear Rams Would Not Have Been Able to Seal the Well, Regardless of When They Were Activated and Regardless of the Position of the Pipe in the BOP
>
> and
>
> There is No Commercially Viable Alternative to the Cameron Shearing Blind Ram That Can Shear and Seal Off-Center Pipe

[Ref. 16, pp. 20, 30] These statements are not possible to reconcile with the fact that a capping stack using Hydril BOP's rams was able to stop the well flow on July 15, 2010. [Ref. 22] Government estimates of well flow and pressure at the time the well was shut in was in excess of 50,000 barrels per day at 6600 psi. [Ref. 17] The rams in the capping stack were very likely subject to a large degree of potential flow erosion during closure, and they sealed, so then why would the Deepwater Horizon BSR, not subjected to erosion up to the time of Autoshear[7], not seal if the pipe was centered?

[6] Furthermore, at the time of AMF triggering, flow up the annulus was being blocked by a VBR, and thus no erosion was taking place at this time from annular flow.

[7] At AMF triggering, the BSR was not activated and was still fully open, so even if some annulus flow developed over time after and up to Autoshear, the BSR blocks would not significantly erode.

3.6. THE DEEPWATER HORIZON BSR HAD POOR ABILITY TO CENTER PIPE, ESPECIALLY IN COMPARISON TO OTHER DESIGNS

Attachment 3 outlines, step by step and with all assumptions, a basic analysis of pipe centering by BSR blades in the presence of friction, when a cut takes place. Ideally, when BSR jaws begin to close, the tangential forces on the pipe at blade contacts would overcome opposing tangential friction forces developed, and push the pipe towards the center of the well bore.[8]

Figure 10 shows the resulting centering forces found, as a function of blade-on-pipe friction coefficient, for the existing Deepwater Horizon BSR (single V blade, 10 degree angle), a double-V BSR with the same blade angle, and another hypothetical double-V BSR with 3 degrees steeper blades. In this plot, negative centering force indicates the pipe will not slide, but rather stick.

A mildly surprising result is that the single V design will not slide the pipe at all if the friction coefficient is greater than about 0.09. This coefficient is lower than a typical dry steel on steel friction coefficient of 0.74 and lower than a reported lubricated steel on steel coefficient of 0.23 (lubricated with light mineral oil), and lower than steel on steel lubricated with castor oil - 0.15. [Ref. 18] At normally expected friction therefore, the pipe will stick and not center. Granted, the presence of fluids can help lubricate the contact and lower the friction, but once the blade digs in, that may not be significant. Also, the oil lubrication effect would be lesser as the blade roughness increases. It is admitted that knowledge of the friction is not good, but this friction limit is at the very least not comforting.

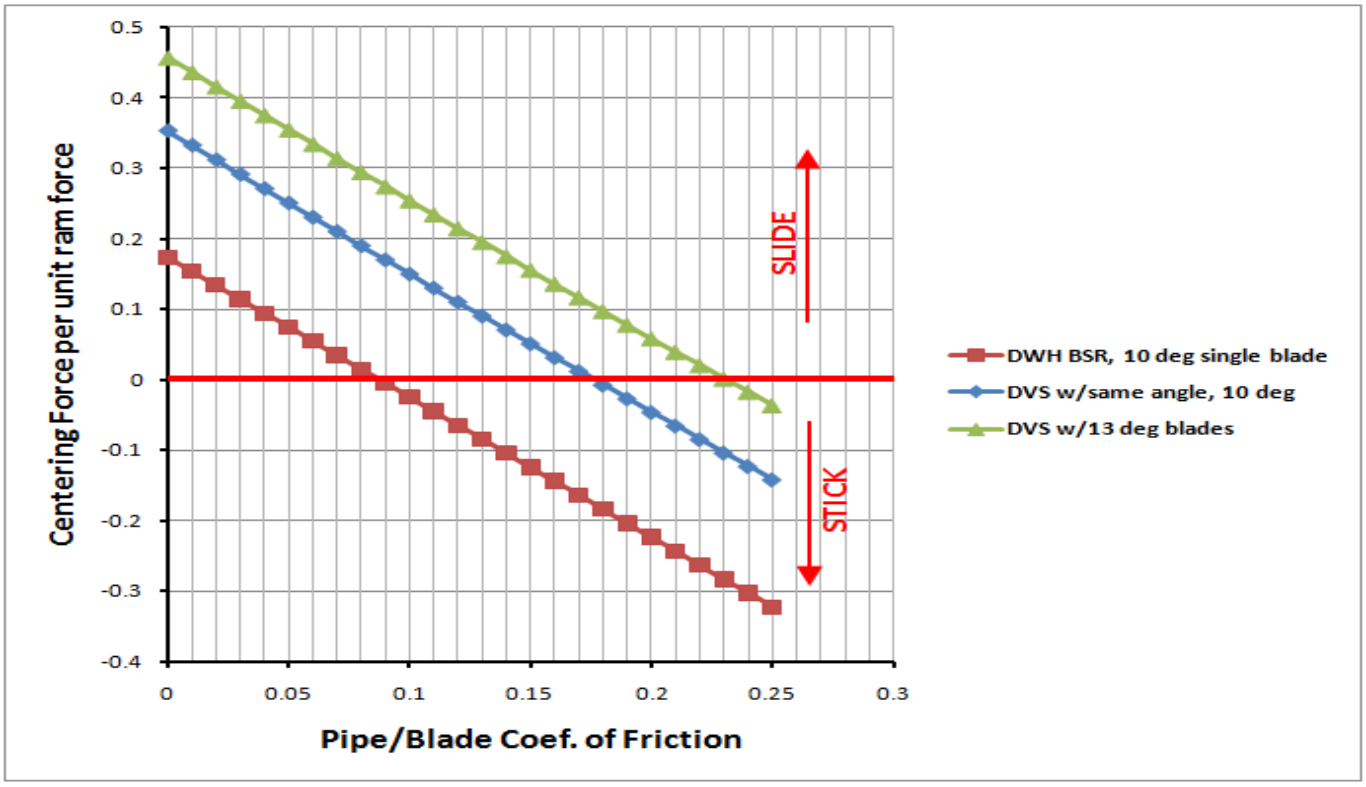

Figure 10. Centering Forces for variable friction and BSR blade design

[8] This analysis is only relevant for a substantially offset pipe. If the pipe is centered at the time of AMF triggering, which we believe to be true, the pipe is already nearly centered. But if later the pipe is pushed to a large offset, then this analysis is pertinent.

In contrast, the comparable double-V BSR design can tolerate a friction coefficient of up to 0.18 before sticking the pipe. This level is much more feasible to envelope steel on steel in the presence of lubrication of different levels (mud, water, or HCs), or none. In addition, the centering force for the double-V at a given friction coefficient is about double that of the single-V, which is not surprising. And increasing the blade angle 3 degrees increases the sticking friction level to 0.23 and the centering force another 30% over the double-V design.

These basic calculations, although not sophisticated, do indicate the approximate relative magnitude of centering improvement for a double-V design over a single-V design, and shows that limiting friction to stick the pipe is not favorable for the single-V design.

3.7 THE MISWIRED 103Y SOLENOID WAS POSITIVELY FAULTY AND PREVENTED AMF OPERATION FROM THE YELLOW POD

Solenoid 103Y and 3AY were miswired as noted in our previous report, which is an unquestionably faulty condition, proven by approximately 25 PETU-based tests (properly interpreted for true PETU signal outputs, see Attachment 2) and additional bench tests showing non-function of the solenoid when the redundant coils (one reverse wired) are simultaneously energized. Transocean's own solenoid rebuilding procedure recognizes miswiring as a fault that would be detected using a simultaneous coil energization checkout test that was never done on these solenoids after their refurbishment. [Ref. 10]

Cameron also mentions problems with these valves when miswired in bulletin FPR # 226314 concerning testing performed on the subject valves. [Ref. 14] Quoting their conclusion:

> It is evident that reverse polarity between Coil A and Coil B in a 223290-63 solenoid valve will not allow it to properly function with both coils energized. Reversing the polarity creates opposing magnetic fields with a canceling affect. It is vital to check function with both coils activated. This step is in the solenoid test procedure X-065393-05, and was in the procedure during the assembly and testing time of the solenoids on the DrillMax 2 Spare Pods. In addition, the power saving software installed on the SEM plays a vital role in producing the pulsation in a solenoid with reverse polarity. It is possible this did not show up on our valve test stand at first pass because those solenoids are fed a constant 24V.

There are, however, two AMF test results with the miswired solenoid 103Y, in which the solenoid appeared to function. [Ref. 11] In another AMF test, there was only partial function that would fail to close the BSR fully, and is thus a failed AMF test. [Ref. 11] Lack of synchronization of coil excitations is the likely cause of these inconsistent AMF test results. It appears that PETU-based tests provide closer synchronization of the coil signals to result in failed valve shifting, but AMF tests, where individual AMF cards are acting independently, can generate larger phase differentials between coil signals that can result in inconsistent test results, some apparent successes and some failures.

Based on these two tests, Mr. Childs contends that the original solenoid 103Y would have fired during AMF because the pulsating PWM signals from SEMs A and B are not synchronized and when out of phase there will still be a resultant magnetic force capable of shifting the valve. [Ref. 2, pp 31-32] The report by Arthur Zatarain, offered by BP, includes a description of how PWM excitation of the magnetic fields, with one coil miswired, can result in some net magnetic field when the pulsating signals are out of phase with each other and might develop a force capable of shifting the valve. [Ref. 12, Appendix A-4] However, this force will always be less than half the force that could be produced if the coils were wired properly and the fields were additive. In addition, the signals from each SEM are independent of each other and random in phase, meaning they could be anywhere from perfectly in phase to 180^{o} opposed. The

resulting magnetic force, therefore, can vary from nothing to approximately the maximum force developed when a single coil is energized.

About 42 tests at Michoud, either PETU-based or bench-based (not AMF tests), showed that the original 103Y Solenoid with the miswired coils failed to operate with both coils excited, and operated properly with only one coil excited.[9] See Attachment 2 for details.

PETU-based tests before AMF testing at Michoud all resulted in Solenoid 103Y failure when both coils were excited. The valve only operated after it had been re-installed once the AMF function had been successfully operated using the replacement 103Y. Even then, on the first test, pressure was not observed until 43 seconds had passed after the AMF was initiated instead of the normal 20 second interval, leaving only 7 seconds of time during which the valve was open, not enough to close a BSR. [Ref. 11] Childs explanation of the tests is misleading, "… it did consistently operate during every AMF cycle" and "[t]he AMF functioned as designed each time, …". [Ref. 2, pp. 31, 32] The observed delay could be caused by some phase mismatch developed over time, whereas the signals started synchronized at the proper time, or could indicate a sticky valve that was working loose with every shift attempt. Contamination was found in the valve during Phase II inspection. [Ref. 13] Contrary to Childs' conclusion that the 103Y solenoid consistently functioned as intended, the most likely scenario for the valve finally shifting at this time is the combination of previous attempts to operate it, the effects of jostling the valve during removal and re-installation, along with the random coincidence of the SEM signals being out of phase later in time but not at the beginning.

Valves become "sticky" or hard to shift when silt or contamination builds up around the moving and sealing components (spools, push pins, etc.). Elastomeric seals may also tend to swell or take a set over time. This problem is much more common in applications where valves function infrequently. Frequent use results in flow through the valve flushing contamination and silt out, but in the case of the high pressure blind shear valve, actuation would be very infrequent, on the order of at least several weeks between shifts.

We believe the solenoid firing late during the first AMF test at Michoud on March 3, 2011 is the first time it activated since installation and lowering to the ocean floor in February, 2010, and it very likely could not have activated the Blind Shear Ram on April 20, 2010. This was a defective solenoid that would never have been installed on the pod if proper maintenance procedures had been followed.

We also note that the later two tests of apparent proper operation of solenoid 103Y may not have been proper after all. The sensing of pressure on the circuit when the valve opens requires the circuit to be dead-headed at or beyond the gage. Once the valve opens due to coil signals out of phase, the pressure is seen. If the magnetic field phasing changed after opening, the valve may have closed or chattered, and a difference in pressure would not have been detected. So the true result of those two AMF tests, in terms of BSR activation time, are not known.

In summary, Childs' contention that Solenoid 103Y functioned because alternating pulsating signals from the SEMs correct for the mis-wired coil scenario is unsupported. The facts are: 1) there is no guarantee that the signals will be phased in a manner that results in any shift force at the desired time, 2) shifting forces developed can only be as high as half that delivered by two correctly wired coils working in tandem, and will usually be less than that, and 3) the lower force available may not be enough to shift a

[9] There was a single test reported to be proper operation with both coils excited. The reason for this anomaly is unknown.

sticky valve. Furthermore, that the AMF failed to function the BSR is confirmed by our analysis of where the drill pipe would have been located at the time of AMF, nearly centered as described above.

3.8. THE BLUE POD 27 VOLT BATTERY WAS POSITIVELY DEPLETED AND PREVENTED AMF OPERATION FROM THE BLUE POD

Childs' attempts to prove that the 27V battery on the Blue pod was not depleted at the time of the incident on April 20, 2010, but rather that the 27V "drained or drained itself" when a low 9V battery in the Blue pod triggered a "cycle that attempted to activate the process every three minutes, reducing battery charge each time." [Ref. 2] However, these conclusion are unsupported for several reasons.

First, Childs places some importance on an AMF card not disarming during AMF tests at Michoud, for proving that the that the 9V battery was insufficiently charged such that it would trigger a rebooting sequence. [Ref. 2 p. 35] However, the AMF card left in an armed state is not necessarily indicative of a problem with the 9V battery. Zatarain's further investigation reported that the 27V battery participates in sending disarm signals. [Ref. 12]

Second, Childs ignores the state of the Yellow pod batteries. Childs writes "Testing of the Yellow pod batteries show that, upon retrieval, the Yellow pod's batteries had sufficient charge to operate the AMF cycle. Further testing at Michoud Phase I and II show the batteries had sufficient charge to operate the AMF in continued testing." [Ref. 2 at 36] We agree. It is also true that the Blue pod 9V batteries were both always better in voltage and loaded performance (tested late in Phase 2) than the Yellow pod batteries. Yet, the 27V battery in the Yellow pod was not depleted. If a low 9V battery could explain the depleted 27V battery in the Blue pod, given that the Yellow pod batteries were consistently more discharged, according to Childs' theory, the 27V battery in the Yellow pod would also have to be depleted. This was not the case.

All measurements of the Blue pod 27 V battery pack yielded low voltages indicating this battery was very depleted. All valid measurements of the Blue pod 9V batteries yielded voltages greater than those in the Yellow Pod 9V batteries, indicating the Blue pod 9V batteries were sufficiently charged.

Table 1 shows no-load test results for times that all the batteries were tested at approximately the same time. The lowest Blue pod 9V battery voltage recorded is always higher than the highest Yellow pod voltage recorded.

Tables 2 and 3 show loaded voltage and current data. The voltages and currents recorded for the Blue pod 9V batteries were always greater than for the Yellow pod batteries.

Third, the 9V batteries in the Blue pod never tested below the purported "drop out" voltage of 5V, that Childs claims will begin the re-booting sequence. [Ref. 2 at p. 35] Loads of 100 ohms, 20 ohms, and 1.6 ohms yielded voltage readings of greater than 5 volts on Blue pod SEM 9V batteries. Necessary drop-out conditions reported by Childs were not present.

Thus, maintaining an argument that a Blue pod 9V battery was low at the time of the incident is inexplicable. There is no reason to believe any scenario that rebooting due to a low 9V battery drained the 27V battery. The Blue pod 27V battery was positively depleted, and the Blue pod 9V batteries were not.

Lastly, Childs' report relies on testing conducted by West and Transocean. [Ref. 2] However, Childs' report does not provide any test procedures or results regarding this testing, nor are there citations to documents containing this information. A set of tests conducted on November 3, 2010, has been identified to us as being relevant to the report. [Ref. 24] However, these documents also do not contain sufficient information regarding the testing protocols and procedure to judge their reliability. Additionally, we have seen no other documentation that such a rebooting sequence occurs.

	NASA Michoud	
Battery	Feb. 28, 2011	June 15, 16, 2011
Blue Pod Batteries (volts)		
SEM A 9 V	8.90	8.92
SEM B 9 V	8.68	8.73
27 V	1.10	2.10
Yellow Pod Batteries (volts)		
SEM A 9 V	8.67	8.58
SEM B 9 V	8.44	8.32
27 V	28.15	28.08

Table 1. No-load battery voltage test results. [Ref. 25]

	NASA Michoud	
Battery, Load, Time, Temperature	Phase 1	Phase 2
Blue Pod Batteries (volts)		
SEM A 9V 100 ohm for 2 min at ambient	8.58	
SEM A 9V 20 ohm for 2 min at ambient	8.24	
SEM A 9V 1.6 ohm for 75 sec at ambient		7.11
SEM A 9V 1.6 ohm for 75 sec at subsea temp		6.62
SEM B 9V 100 ohm for 2 min at ambient	8.39	
SEM B 9V 20 ohm for 2 min at ambient	8.02	
SEM B 9V 1.6 ohm for 75 sec at ambient		6.79
SEM B 9V 1.6 ohm for 75 sec at subsea temp		6.35
Yellow Pod Batteries (volts)		
SEM A 9V 100 ohm for 2 min at ambient	8.30	
SEM A 9V 20 ohm for 2 min at ambient	7.99	
SEM A 9V 1.6 ohm for 75 sec at ambient		6.88
SEM A 9V 1.6 ohm for 75 sec at subsea temp		6.34
SEM B 9V 100 ohm for 2 min at ambient	8.08	
SEM B 9V 20 ohm for 2 min at ambient	7.63	
SEM B 9V 1.6 ohm for 75 sec at ambient		2.41
SEM B 9V 1.6 ohm for 75 sec at subsea temp		1.76

Table 2. Loaded battery average voltage test results. [Ref. 26]

	NASA Michoud	
Battery, Load, Time, Temperature	**Phase 1**	**Phase 2**
Blue Pod Batteries (amps)		
SEM A 9V 100 ohm for 2 min at ambient	**na**	
SEM A 9V 20 ohm for 2 min at ambient	**na**	
SEM A 9V 1.6 ohm for 75 sec at ambient		**4.281**
SEM A 9V 1.6 ohm for 75 sec at subsea temp		**3.982**
SEM B 9V 100 ohm for 2 min at ambient	**na**	
SEM B 9V 20 ohm for 2 min at ambient	**na**	
SEM B 9V 1.6 ohm for 75 sec at ambient		**4.093**
SEM B 9V 1.6 ohm for 75 sec at subsea temp		**3.825**
Yellow Pod Batteries (amps)		
SEM A 9V 100 ohm for 2 min at ambient	**na**	
SEM A 9V 20 ohm for 2 min at ambient	**na**	
SEM A 9V 1.6 ohm for 75 sec at ambient		**4.142**
SEM A 9V 1.6 ohm for 75 sec at subsea temp		**3.817**
SEM B 9V 100 ohm for 2 min at ambient	**na**	
SEM B 9V 20 ohm for 2 min at ambient	**na**	
SEM B 9V 1.6 ohm for 75 sec at ambient		**1.446**
SEM B 9V 1.6 ohm for 75 sec at subsea temp		**1.049**

Table 3. Loaded battery average current test results. [Ref. 27]

IV. CONTRIBUTIONS TO THIS REPORT

Dr. Rory R. Davis, P.E.

I contributed to the following sections in this report: I, II, III (all subsections), IV, V, and VI (Attachments 1, 2, 3, 4).

Patrick R. Novak, PE

I contributed to the following sections in this report: 3.3 (items 6 and 12), 3.5, 3.7

Dr. J Neil Robinson

I contributed to the following sections in this report: 3.2, 3.3, 3.7, 3.8

Raymond Merala, MS, PE

I contributed to the following sections in this report: 3.8

V. REFERENCES CITED

1. Transocean, *Macondo Well Incident – Transocean Investigation Report, Volume 1 and Volume 2*, June 2011. In particular, see *Appendix G – Hydraulic Analysis of Macondo #252 Well Prior to Incident of April 20, 2010.*
2. *Expert Report of Greg Childs*, September 23, 2011.
3. Transocean, *Macondo Well Incident – Transocean Investigation Report, Volume 1 and Volume 2*, June 2011. In particular, see *Appendix M – Structural Analysis of the Macondo #252 Work String.*
4. Det Norske Veritas, *Final Report for United States Department of Interior – Forensic Examination of Deepwater Horizon Blowout Preventer, Volume 1 and Volume 2*, March 30, 2011 see pages 150-154; Kenney, G.D., *Forensic Examination of Deepwater Horizon Blowout Preventer – Addendum to Final Report*, Det Norske Veritas, April 30, 2011 (DNV Report #EP030842, Contract #M10PX00335), see pages 10-14.
5. *Expert Report of Forrest Earl Shanks II*, October 17, 2011. In particular, see *Appendix C - Calculation of vertical friction on 5-1/2" Drill Pipe in 6-5/8" - 3-1/2" Variable Bore Pipe Rams (VBRs).*
6. *Expert Report of Forrest Earl Shanks II*, October 17, 2011.
7. Timeline Regarding Specific Events Concerning the BOP, August 1999 – May 30, 2010, (BP-HZN-BLY00087028) see page 9.
8. LeNormand, William, *Daily Report Sheet – Subsea Pod Intervention*, Cameron Controls, May 5, 2010, (CAM_CIV_0029724 - CAM_CIV_0029744) see page 13.
9. *Expert Report of Greg S. Perkin, P.E.*, October 17, 2011.
10. Ankrom, J., *Transocean Technical Information Bulletin OPT-TIB-435-01: Instructions for Rebuilding Cameron Controls Solenoid Valve -Family 435*, September 9, 2002, (Ex. 3798) (TRN-MDL-01547899 - TRN-MDL-01547905).
11. Det Norske Veritas, *DNV SEM Notebook*, pp. 016888 to 016898, March 3-4, 2011 (Ex. 3130).
12. *Expert Report of Arthur Zatarain, P.E.*, October 17, 2011.
13. Det Norske Veritas, DNV IMAGE 23117.
14. Cameron, *Report of Findings re: FPR # 226314* (Ex. 5165); Picture of Disassembed Solenoid Valve (Ex. 3781).
15. *Expert Report of Cliff Knight, P.E.*, October 17, 2011.
16. *Expert Report of David L. O'Donnell*, October 17, 2011.
17. National Commission on the BP Deepwater Horizon Oil Spill and Offshore Drilling, *Report to the President*, January 2011. See particularly, Ch. 5, pp. 161-167.
18. T. Baumeister, et. al, *Marks' Standard Handbook for Mechanical Engineers*, Fuller, Dudley, D., "Friction", in Section 3 - Mechanics of Solids and Fluids 8th Edition, pg. 3-26, Table 1 (Coefficients of Static and Sliding Friction).
19. BP, *Deepwater Horizon Accident Investigation Report*, September 8, 2010, (BP-HZN-BLY00144940 - BP-HZN-BLY00145180).

20. Deposition of David McWhorter, July 7, 2011 at 233:19-234:25 (Vol. 1); Deposition of William LeNormand, June 21, 2011 at 143:10-144:25 (Vol. 2).

21. Steve Myers, Re: DWH-BOP follow up, Email, November 3, 2010, (TRN-INV-01834164 - TRN-INV-01834165)

22. BP, *Macondo 252 Well Integrity Test*, July 11, 2010, (TRN-MDL-02488242-268).

23. LeNormand, William, *Daily Report Sheet – Subsea Pod Intervention*, Cameron Controls, May 5, 2010, (Ex. 3602), (CAM_CIV_0046703 - CAM_CIV_0046705).

24. SEM Testing at WEST DEC, November 3, 2010, (TRN-INV-01130032 – TRN-INV-01130041); Mika Reed, November 17, 2010, Email, (TRN-INV-02546919 - TRN-INV-02546939).

25. Dugal-Whitehead, N., *Test Preparation Sheet - Test of Deepwater Horizon Blowout Preventor Battery Voltages*, Feb. 28, 2012 (sic 2011), DNV Phase 1 Test Data; Dugal-Whitehead, N., *Test Preparation Sheet - Test of Blue SEM Batteries*, June 15, 2011, DNV Phase 1 Test Data (DNV2011061502); Dugal-Whitehead, N., *Test Preparation Sheet - Test of Yellow SEM Batteries*, June 16, 2011, DNV Phase II Test Data, (DNV2011061601-603).

26. Expert Report from R. R. Davis, "Deepwater Horizon Blowout Preventer Examination and Testing", Appendix A, Figure A-3, Average voltage measured during "loaded" tests of 9 volt batteries; Table A-1, Loaded battery summary data from Test Preparation Sheet, Test of Deepwater Horizon Blowout Preventor Batteries - Yellow, March 1, 2011, prepared by Norma Dugal-Whitehead, DNV Test Data, Phase I; Test Preparation Sheet, Test of Deepwater Horizon Blowout Preventor Batteries - Blue, March 1, 2011, prepared by Norma Dugal-Whitehead, DNV Test Data, Phase I.

27. Expert Report from R. R. Davis, "Deepwater Horizon Blowout Preventer Examination and Testing", Appendix A, Figure A-5, Average current measured during 9 volt "loaded" battery tests; Table A-2, Summary of Full Load Battery Testing compiled from DNV2011062203- Battery Testing Summary.xls, and test data files listed under "File Name".

28. Blevins, R.D., "Applied Fluid Dynamics Handbook," van Nostrand Reinhold Co, 1984.

29. DNV, *Summary Preparation Sheet BOP-009 Test Solenoid at Deep Sea Temperature*,May 16, 2011, DNV Phase II (DNV2011051601); Anon., *Summary Preparation Sheet BOP-010 Test Solenoid at Deep Sea Temperature and Pressure*, May 18, 2011, DNV Phase II (DNV2011051801); TPS_BOP-10_*Summary_Test_Solenoid_at_Deep_Sea_Temperature _w_Hydraulic_Pressures.pdf*, within "BOP Data Files by Test Date Initiated", Phase 2 KPMG web site, 05-18-2011 folder (DNV2011051801).

VI. ATTACHMENTS

ATTACHMENT 1. DRILL PIPE FORCE CALCULATIONS

Flow Forces Pipe Loading

The apparent error in SES's flow force analysis of their Appendix G [1] was pointed out in the body of the report, which makes flow force analysis in their Appendix M [3] also erroneous. We now describe flow force calculation methods used for a fresh look at the question. All details of the flow equations are obtained from [Ref. 28].

The Darcy-Weisbach formula allows calculation of delta p (aside from gravity head) for a flowing pipe or duct:

$$\Delta p = p_d \, f \, L / D \qquad [1]$$

Where p_d is the dynamic pressure or $\frac{1}{2}\rho U^2$, and U is most often taken as the mean volumetric flow rate in the duct, and ρ is mass density. D is the hydraulic diameter of the duct, L is duct length, and f is the Moody friction factor.

The fluid shear stress at the wall (or surface traction) is

$$\tau = p_d \, f / 4 \qquad [2]$$

In the case in question, flow is not laminar, but rather is "transitional" or possibly fully turbulent at the highest Reynolds numbers we will see. A "transitional" friction factor curve fit is appropriate in this case (full turbulent curve fits give slightly lower friction factors at high Raynolds numbers). This curve fit is within about 5% of the Colebrook-White correlation, based on experimental data. The curve fit is:

$$f = 1/[\, 1.14 - 2 \log_{10}[\, e/D + 21.25/(Re^{0.9})]^2 \qquad [3]$$

where e is surface roughness, D is hydraulic diameter, and Re is Reynolds number, which is:

$$Re = UD/\nu \qquad [4]$$

and ν is the kinematic viscosity of the fluid.

The flow delta p affects pressure change along the pipe, and in addition the shear stress imposes surface traction on the pipe of τ times the wetted surface area.

With the drill pipe vertical, we use Bernoulli's law to account for fluid head delta p and the flow delta p as a function of elevation. We assume mass flow rate to be constant in the casing/pipe annulus, assuming no leaks, so we can calculate average flow velocity at any point by simple area ratio from one known point to another. The first known point is based on an assumed known mass flow rate and a fluid density.

Hydrostatic Pressure Pipe Loading

As will be explained in detail below, the pressure x area (pA) forces on the drill pipe are also erroneously handled in SES's analysis [Ref. 3], so results for their "VBR" case are also incorrect.

It is useful to return to first principles to explain loading on the drill pipe. The only way to impose force on the pipe is 1) surface normal pressures inside, outside, and at ends, 2) surface tractions tangential to the surface, and 3) self-weight of the pipe wall under gravity. Rams or annulars, or wellbore contacts may impose local normal pressures or tractions, so that falls within items 1 and/or 2. Buoyancy is a manifestation of normal pressure forces, falling within item 1.

Moving on to consideration of pA forces, some assumptions in Reference 3 about the work string loading conditions are erroneous. The "VBR" pressure load case does not make sense in light of basic engineering mechanics. There cannot be an abrupt change in force within the pipe at the VBR, simply due to delta p across the VBR. And in addition, the VBR is assumed by them to not be able to hold any axial load on the pipe. Therefore, VBR surface tractions are assumed negligible and net vertical force due to VBR clamping is negligible. VBR normal pressures are just that, normal, so do not impose vertical forces.

We must consider the three pipe sizes of the drill string when properly considering pipe forces. First, there is a slug of fluid with the diameter of the lowest 3-1/2" string that extends from the bottom end of the string (assumed open) to the very top at the rig (pipe assumed closed and pinned here). This slug only generates pA force on the drill pipe top cap, equal to the surface drill pipe pressure times the section area of the slug, which has a diameter of only 3". This force is inconsequential to the pipe, because it is directly reacted at the pin holding the drill pipe. It does not serve to compress or stretch the drill pipe anywhere. This pA force of about 40 kip for Reference 3's VBR load case is directly reacted to the rig, and would be seen in the hook load, but not in pipe wall tension or compression.

The most obvious axial load on the pipe is pA force at the lower open end of the string. However, this force is not over the full OD pipe area, as assumed by SES, it is only over the wall thickness annulus of the 3-1/2" pipe. This force compresses the pipe for some distance from the end, until pipe weight tension overtakes the pA force.

Additional vertical net forces are possible at the two changes in pipe size, see Figure 1-1. The projected areas, inside and outside, are not necessarily equal, and the pressures inside and outside are not either (due to mud weights, HCs, etc), so the net force will not be zero at these transitions. The net force could be compressive or tensile on the pipe, depending on the conditions.

Note that these size change point forces account for all fluid in the pipe aside from the long I.D. slug mentioned before, because the local pressures include the fluid column heads. Buoyancy is effectively included by the size change forces and the end pA force.

At pipe joints, we assume that the pressure change along one joint length is not significant, and projected area is the same above and below a joint, so net force is zero, internal or external.

The self-weight of the pipe wall is uniformly distributed along the length of the pipe, according at any point to the pipe size in question. No fluid weight is included, as it has already been considered via the pipe size change point forces (via local pressures).

The SES report erroneously includes all internal fluid weight in the pipe force calculation. [Ref. 3] The report also erroneously applies the bottom end pressure over the whole OD cross section, instead of just the wall thickness annulus. In addition, the net size change forces are not considered at all. If they were, the force graphs, for example Figure 8, would show step changes in force at the pipe size change points. Instead, a large change in axial force is shown at the VBR, although there is no pipe surface normal to axial to develop any force with fluid pressure. And, the VBR is assumed to not impose axial force, by their assumption. Thus, the assumed effective tensions are incorrect by a great amount. In reality, the effective tension should decrease with depth, smoothly through the VBR, but with some substantial steps at the pipe size change points. The size changes should also be remembered when considering the force levels and stresses in the respective size segments.

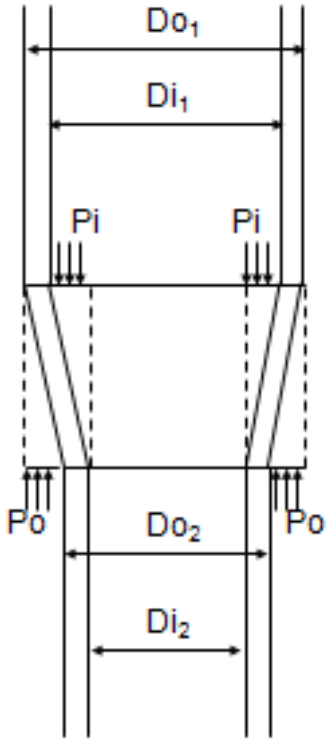

$$dFi = 0.25\,\pi\,(Di_1^2 - Di_2^2)\,Pi \quad \text{(positive downward)}$$
$$dFo = 0.25\,\pi\,(Do_1^2 - Do_2^2)\,Po \quad \text{(positive upward)}$$

Figure 1-1. Differential annulus forces at a pipe size change

Re-Calculated Pipe Forces

The desire is to maintain "apples and apples" with some of the more reasonable parameters of the TO analysis, to allow for a direct comparison of forces. The first case will be wellbore flow just before VBR closing. SES quotes, for this "Scenario 2", a maximum blowout flow rate of 60,000 STB/day, and they also convert that to a mass flow rate of 22,299 lbm/day, which upon some checking seems reasonable. [Ref. 1 at p. 144] So we use that mass flow rate as input to our analysis.

We also use SES stated density and viscosity of the HCs for pressures of 2000 and 5000 psi, presumed to account for the supercritical nature of the fluid under pressure. [Ref. 1 at p. 142] The data for HC properties are (0.525 g/cc density and 0.4 cP viscosity) at 5000 psi and (0.307 g/cc density and 0.6 cP viscosity) at 2000 psi, both at 170 °F. Here, the viscosity is "dynamic", not kinematic and appropriate conversion is made using the density. We interpolate and extrapolate these points assuming linearity for our analysis.

At that time, we have a wellhead pressure measurement of 1174 psi (estimated from graphs in Reference1, p. 111), and the pipe is assumed filled with sea water. In different places, SES may have used a different assumption, sometimes with 12 bbl of HC in the bottom of the string, but we use the simpler case. At the bottom end of the drill pipe, the annulus static pressure is the same as the pipe's, and calculates out to 4890 psi (static head only down the pipe).

The drill pipe roughness is taken as 0.02", which is on the high end for "light rust or small deposits" in the fluid dynamics handbook. [Ref. 28] Given that the pipe is washed by HCs, this is likely a conservatively rough estimate. For "smooth pipe in good condition" the factor would be 0.004".

Using all these inputs and the methodologies described above, we perform a conservative piecewise analysis along the pipe, from bottom to top. It is conservative in the respect that the properties for a piecewise segment of fluid annulus are taken from the bottom end, resulting in higher pipe forces. This is done in a spreadsheet which is provided along with cited references of this report (the spreadsheet contains all three cases analyzed). For this first case, the pipe force results are shown in Figure 1 of the body of the report.

A second case, shown in Figure 2 of the body of the report, was next run for the conditions at the instant the VBR fully closes and seals.

A third case, shown in Figure 3 of the body of the report, is most instructive to discuss first. In this case, after VBR closure, there is no flow, only hydrostatic pressures. The pressure below the VBR has built up from the time of the second case, and above the VBR the HC's have boiled off gas and reduced pressure. The analysis used SES's assumptions of a) 8500 psi below closed VBR, b) about 500 psi above closed VBR, c) seawater only in the drill pipe, d) 5 ppg HCs in annulus below VBR, and e) 2 ppg HCs in annulus above VBR (assumed constant and not varying as for the first two cases). Axial forces are assumed by SES not to be carried by the UA or VBRs, and we make the same assumption for apples and apples comparison.

For reference, the total metal weight of the drill string is about 245 kip. Thus, the surface pipe tension in Figure 3 indicates the net buoyancy effect of the pipe walls is not very large. The pipe is in tension with about 10 kip at the BOP, far different than determined by SES. [Ref. 3]. The bottom end compressive force of about -24 kip is simply the pA force on the 3-1/2" pipe wall end, for a pipe end pressure of 9362

psi (extrapolated from annulus at VBR depth). Each of the three size pipe sections have different load slopes proportional to their metal lineal weights. At the pipe size transitions, net size change force steps are actually quite large, but for different reasons at each place. At the upper size change, the net force step is mainly due to differential pressure, inner vs. outer, because the wellbore annulus was assumed to have very low pressure and very low density HCs in it. At the lower size change, the net force step is mainly due to area differential, inner vs. outer, but also both pipe and annulus pressures are very high (though near equal).

The newly calculated pipe tension is clearly nothing like SES represents in their Figure 8. [3] One must conclude that using the "equivalent weight" method as in the SES report is not suitable for evaluating pipe tension, although it may have use for some other purposes.

One should note, the zero depth tension from the new calculation is not the net rig holding force (hook force) for the whole string. As the top of the pipe is assumed capped, the rig level pipe pressure (5645 psi) times the full ID area of the top 6-5/8" string would be subtracted to get the net rig force. In this case, the cap force calculates as about 140 kip, so the net rig force is about 96 kip tension. But this has no direct relevance to the pipe tension, as the 140 kip cap load is directly reacted by the rig. ***It is very important to make the distinction between pipe wall tension and hook load.***

One should note, if one assumed heavier and higher pressure HCs above the VBR, the pipe tension would not change below the first pipe size change. Above that it would, but that does not change the force conditions at the BOP. So the assumed annulus conditions above the BOP are irrelevant for pipe tension. Another way of viewing this is that pipe force causality is "bottom up".

A quick check was done where the pipe is assumed completely filled with 5 ppg HCs instead of seawater. The pipe tension differences are negligible, especially near the BOP. There is a little force difference at zero depth, indicative of a little buoyancy difference.

Overall, buoyancy is not a large effect, and is complicated by different weight fluids. If only seawater fluid, the total buoyancy distributed over the whole string would be only about 32 kip, and with HCs, it is substantially less. In contrast, the first pipe size change net force step is about 50 kip.

Drill pipe FEA

We now show some salient FEA results (using the ANSYS FE code).[10] The model includes some length of 5½" pipe above and below the BOP, enough to avoid end effect issues. A thicker tool joint is included just below the UA. Forces on the pipe are applied at both ends, and self-weight of the pipe is assumed included in the applied forces. The fixity imposed on the pipe by UA or VBRs (Upper or Middle) is resettable for each analysis. The BOP wellbore is assumed rigid and fixed. The flex joint is adjustably rotatable, along with the portion of riser attached above it, and both are modeled as flexible (but are very rigid compared to the pipe). The entire model solves in 3-D, including cylindrical contact of the drill pipe with the bore of riser, flex joint, and BOP, and full large deflection nonlinearity, including full kinematic tilting of the flex joint.

In solution plots, deflection and pipe/wellbore geometry are shown at true scale. Some plots show von Mises stress in the pipe with 0-150 ksi color contours. In others, elements are shown with color coding.

[10] Computer files for the analyses are provided with considered references

Short extent of VBRs along the pipe are orange, BSR is magenta, and UA is red just above the tool joint. Of primary interest in results is offset deflection of the pipe at the BSR, and observation of pipe stress levels.

The first case of interest, Case 1, is for AMF time, after the MVBR has closed, and the pipe tension is 36.5 kip or less. We assume the UA restrains the pipe laterally, but not vertically nor in rotation. The MVBR is restraining laterally and vertically, and in rotations. Because pipe force is applied at both ends, the MVBR does not react significant force, however, it is effectively just a datum for axial deflection.

At this time, the rig has just lost stationkeeping. Given the space between the pipe and riser annulus (7.0”), the rig can drift about 50 feet without significantly disturbing the drill pipe centered in the BOP (flex joint tilt of 0.57 degrees). In this case, no analysis is necessary, as the pipe under reasonable axial load would remain virtually straight. So, we next consider a very conservative case of the rig drifting the length of a football field, 300 feet (or an equivalent of drift and sea currents to tilt the flex joint the same amount, it turns out 3.43 degrees at the flex joint). Figures 1-2 and 1-3 show the results of this case for +36.5 kip expected maximum tension loading in the pipe around this time. This case provides the largest lateral deflection of the pipe at the BSR of -0.59” (-X direction, or physically to left in plots), in comparison with other cases checked at +10.5 kip (-0.58”) and 0 kip (-0.57”). Even if one applies -30 kip, the deflection is only -0.54”. So clearly, the pipe is near centered despite the substantial flex joint tilt and possible pipe forces at this time (in fact, the pipe force level has little effect). This is further evidence that the pipe was nearly centered at AMF time. It is also of interest that tension is worse for offset deflection than compression when the VBR holds the pipe. The case of -30 kip represents the implausible case that pre-VBR closure compression is maintained after VBR closure, and actually results in less offset at the BSR.

The next case of interest, Case 2, is for later times and further rig drift to 5 degrees of flex joint tilt. Offset at the BSR increases to as high as -1.14 inches for the -30 kip compression case (although not plausible now, tension is more likely with rig drift), and about 0.2” less for +30 kip tension. Plots are not given, as results appear indistinguishable from Case 1. But this shows that compressive forces cause more offset than tension when the riser is tilted more at later times.

The next case, Case 3, considers a maximum flex joint tilt of 15 degrees, which would occur for 1273 feet of rig drift or drift/current equivalent, or more (and the flex joint bottoms out at about 15 degrees if more). We also assume the MVBR is still tightly closed (though not as likely now, it is analyzeable). Figures 1-4 and 1-5 show the result for +30 kip tensile load (tensile is likely with this much rig drift). We have pipe contact with the wall for a long distance just above the BSR, and offset at BSR of -3.39” just below the contact region. It was also found that the BSR offset is almost identical, and wall contact still occurs for 0 or -30 kip forces. In addition, if one assumed that the UA holds vertically instead of the VBR, the BSR offset is about the same (contact nearby appears to strongly govern). It appears that for the largest flex joint tilt, the tilt dominates and magnitude or sense of pipe force again becomes less influential.

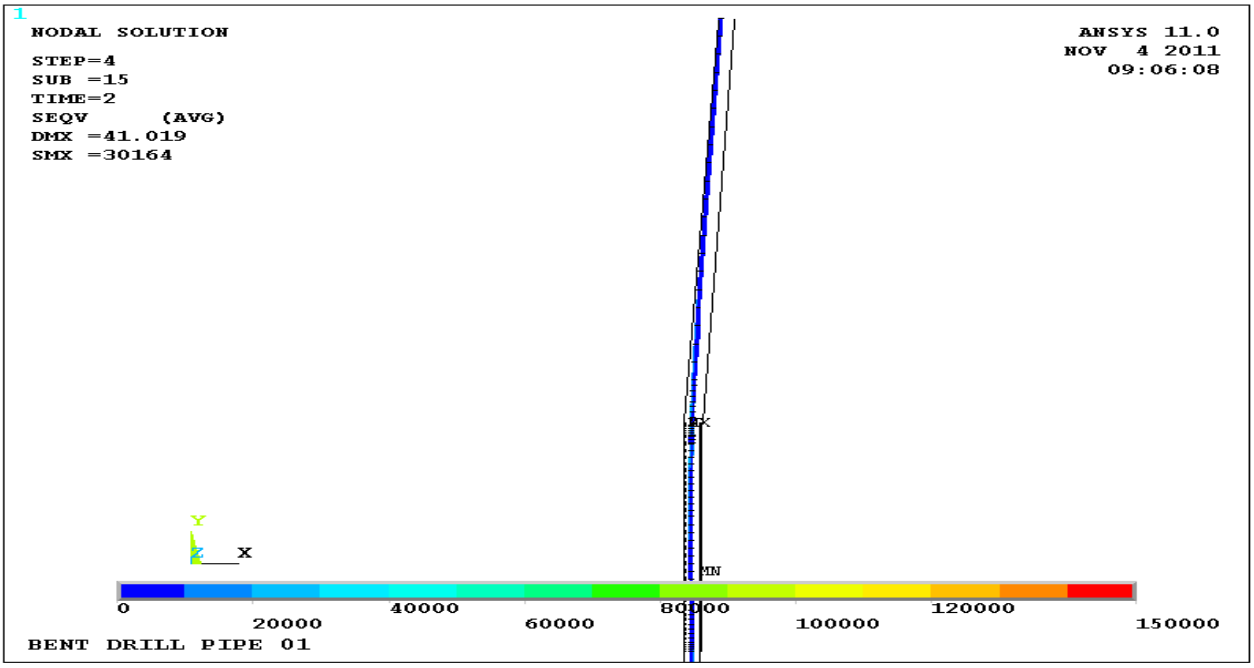

Figure 1-2. Case 1, distant view showing tilted flex joint and riser, and pipe bearing against riser wall (pipe von Mises stress shown in color contours, psi units). Maximum von Mises stress is only 30, 164 psi (neglecting pressure hoop stresses)

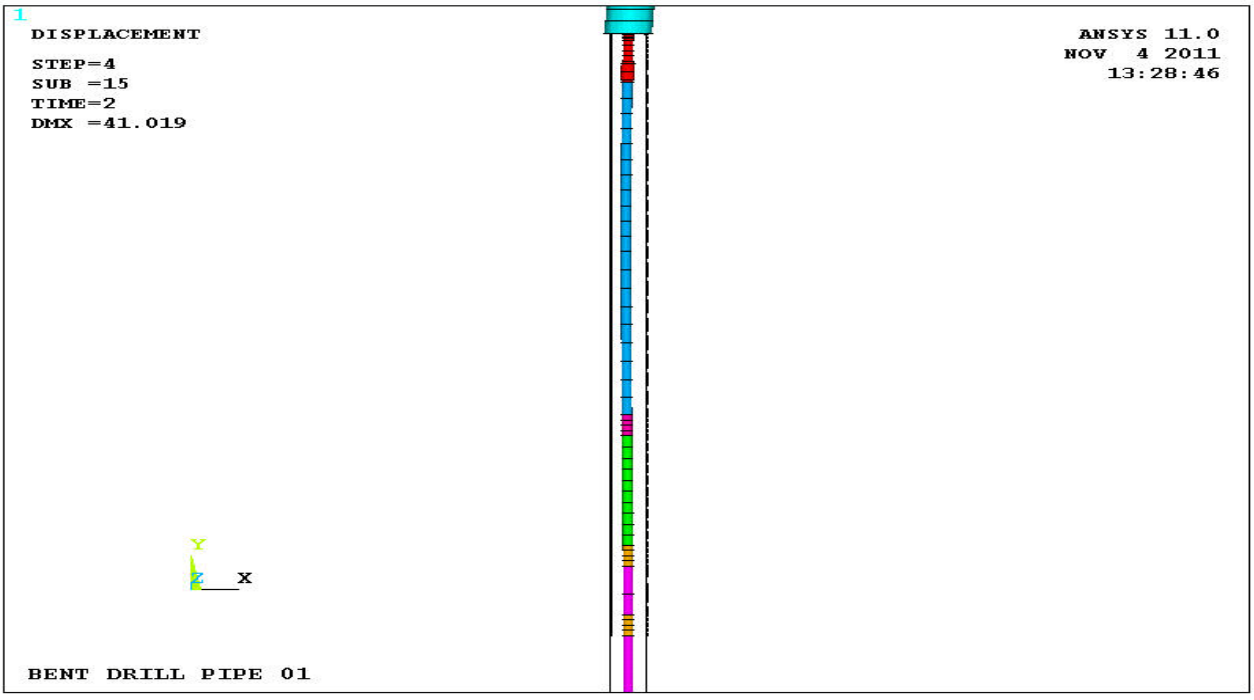

Figure 1-3. Case 1, closer view showing ram locations (Max lateral deflection well above BSR= 1.16", short extent of VBRs along the pipe are orange, BSR is magenta, and UA is red just above the tool joint

However, inevitably, with no hydraulic pressure, the MVBR would loosen enough to allow some rotational, lateral, and possibly even axial freedom to the pipe. This is highly likely to occur with a long period of rig drifting and the pipe working against the closed but unpressurized and unlocked VBR,

sliding up and down and tilting back and forth as the rig drifts. At this later time, axial load is more likely reacted by the rig, not the VBR (nor the UA). Unfortunately, the extent of movement of the pipe in the VBR and the pipe loads at such later times is difficult to know and FEA of hypothetical conditions is guesswork (Cases 1 through 3 were quantifiable). The drill pipe would certainly be more free to move however, and as the FEA results show, riser movement in response to rig drift and/or sea currents is the major determinant of pipe motion in the BOP, and reasonable levels of pipe load are not. One can certainly envision freedom of rotation and some small lateral movement of the drill pipe at the MVBR could allow the pipe to offset substantially more than in Case 3. For example, an exploratory FEA just allowing rotational freedom at the MVBR in Case 3 showed an additional 1.5 inch of offset of the pipe at the BSR.

Finally, note given that the BSR closes when Autoshear is activated, any accumulated looseness of the MVBR, if not too large, would be tightened up after the BSR closure, because then the ST locks would close and push the VBR closed again, although not with full force. Thus the fact that the MVBR was loose before Autoshear could be disguised.

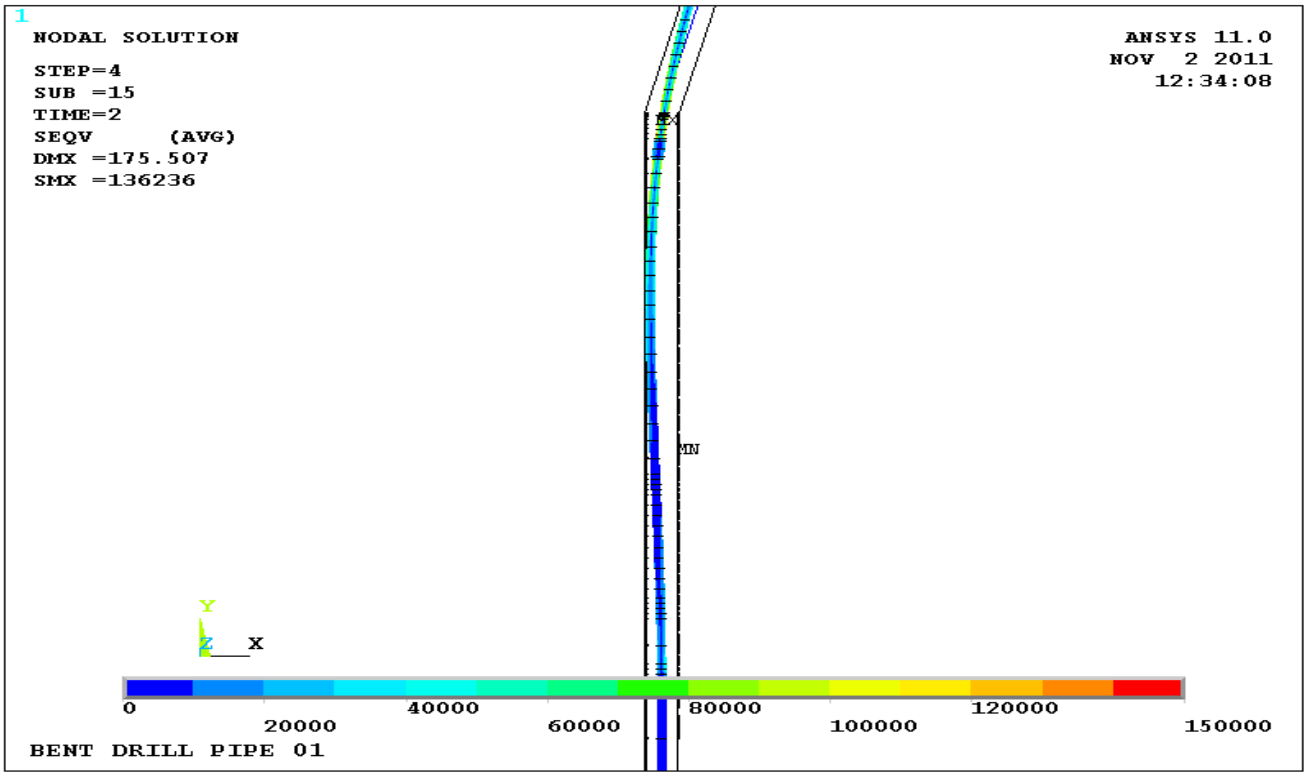

Figure 1-4. Case 3, distant view showing tilted flex joint and riser, and pipe bearing against riser wall (pipe von Mises stress shown in color contours, psi units). Maximum von Mises stress is 136, 236 psi (neglecting pressure hoop stresses)

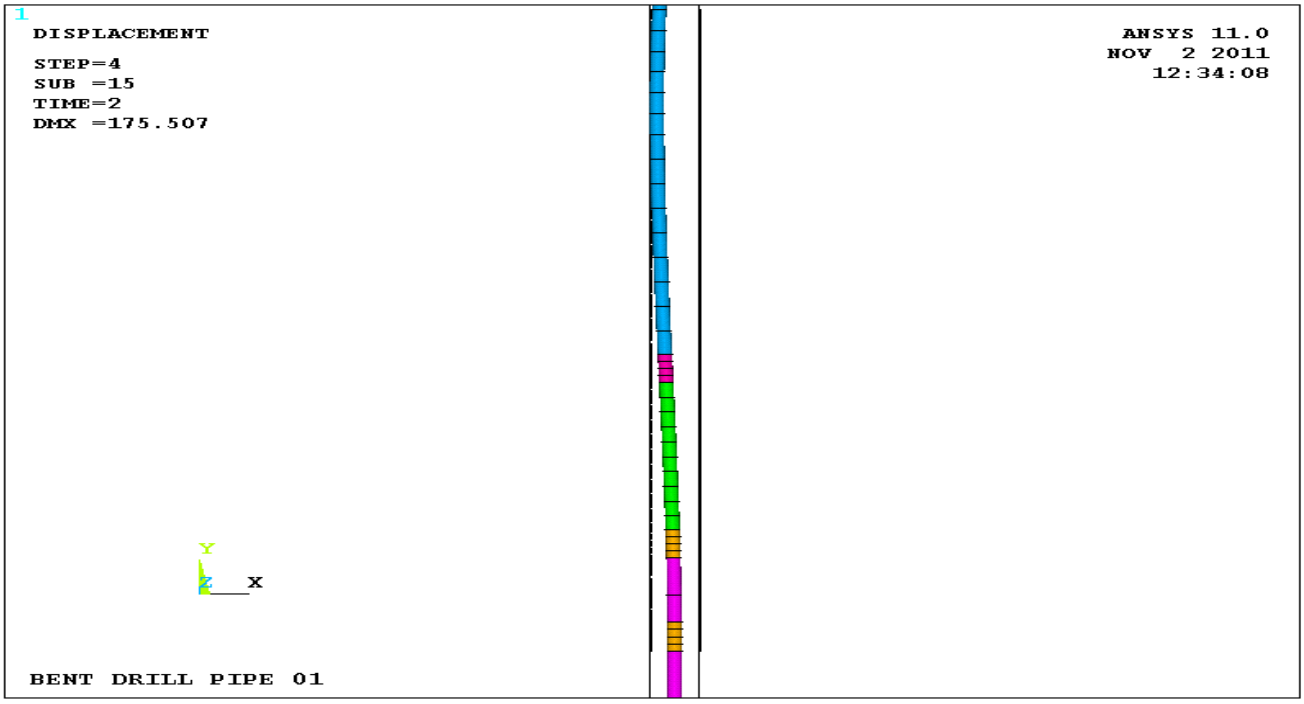

Figure 1-5. Case 3, closer view showing ram locations (Max lateral deflection just above BSR= 6.68", short extent of VBRs along the pipe are orange, BSR is magenta, and UA is red just above the tool joint [but UA not visible in this view])

ATTACHMENT 2. SOLENOID 103Y TESTING SUMMARIES

For PETU-based tests, we have two varieties of PETUs that were characterized in Phase 2 testing at Michoud. One variety has a single switch, indicating SEM A or B, and the other variety has two switches, the one indicating SEM A or B, but another indicating single or dual SEM activation.

In actuality, the single switch PETU, which indicates activating SEM A or B separately, always activates both A and B together. The two switch PETU, which indicates ability to do single A or B or dual A and B activation, always only activates one SEM, A or B, according to the first switch setting alone. These behaviors were conclusively finally established in Phase 2 testing.

There are a total of four PETUs that were used, two in Phase 1 and two different ones in Phase 2, in both cases one of each variety. To avoid terminology confusion in the following tables, the PETU used will be identified by its true ability to activate SEMs, either SINGLE or DUAL.

Phase 1 tests done on Solenoid 103Y or 3AY original before 05-03-2011 were bench tests not performed with PETUs. In these tests it appears single coils were activated, and results showed correct valve switching. The number of tests is not clear in the record. DC power supplies were used to drive the coils.

Table A-1. Phase 1 PETU-Based and Bench Solenoid 103Y Original Test Summary (in chronological order, PETU tests starting 05-03-2011) [Ref. 11, 29]

TEST #	PETU	True A-B setting	Test Result – Shifted?	Comment
1	Bench	A	Yes	
2	Bench	B	Yes	
3	DUAL	A+B	No	
4	DUAL	A+B	No	
5,6	DUAL	A+B	No	“multiple times”, assumed 2
7,8	DUAL	A+B	No	“multiple times”, assumed 2, cleaned pie connector before
9, 10, 11, 12, 13	DUAL	A+B	No	tried A or B, none worked (changed to 103R, worked)
14,15, 16, 17	DUAL	A+B	No	After AMF, tried A or B
18	SINGLE	?	Yes	switch could have been on A or B
19	SINGLE	A	Yes	
20	SINGLE	B	Yes	
21*	DUAL	A+B	Yes	A setting, reported pressure
22, 23, 24	DUAL	A+B	No	B setting, 3 times
25	DUAL	A+B	No	A setting
26	SINGLE	A	Yes	
27	SINGLE	B	Yes	
28	SINGLE	A	Yes	
29	SINGLE	B	Yes	
30	SINGLE	?	Yes	switch could have been on A or B

*This test is anomalous in comparison with others.

In phase 2, no PETU-based tests were done with Solenoid 103Y original. It was found to have shorted wiring after disassembly and re-assembly after AMF testing.

Table A-2. Phase 2 Bench* Solenoid 103Y Original Test Summary (in chronological order, starting 05-16-2011) [Ref. 29]

TEST #	Type	True A-B setting	Test Result – Shifted?	Comment
31	Bench	A	Yes	cold, no pressure
32	Bench	B	Yes	cold, no pressure
33	Bench	A+B	No	cold, no pressure
34	Bench	A	Yes	ambient, no pressure
35	Bench	B	Yes	ambient, no pressure
36	Bench	A+B	No	ambient, no pressure
37	Bench	A	Yes	cold, pressure
38	Bench	B	Yes	cold, pressure
39	Bench	A+B	No	cold, pressure
40	Bench	A	Yes	ambient, pressure
41	Bench	B	Yes	ambient, pressure
42	Bench	A+B	No	ambient, pressure

***Bench tests used DC power supplies to drive the coils.**

Table A-3. Phase 1 AMF Yellow Pod Solenoid 103Y Original Test Summary (in chronological order) [Ref. 11, 29]

TEST #	Type	True A-B setting	Test Result – Success?	Comment
A	AMF	A+B implied	No	103Y fired 23 sec late, 7 sec stayed open (inadequate for BSR close)
B	AMF	A+B implied	Uncertain	Apparent full duration, but did not look for valve chatter
C	AMF	A+B implied	Uncertain	Apparent full duration, but did not look for valve chatter

***Bench tests used DC power supplies to drive the coils.**

ATTACHMENT 3. BSR PIPE CENTERING CALCULATIONS IN THE PRESENCE OF FRICTION

We consider a general 2-blade cut on a pipe section with blade normal and tangential friction forces, neglecting all other external forces on the pipe except a force **P** which can hold the pipe against sliding, at equilibrium. If the force **P** is positive at equilibrium, the pipe would slide toward the center of the cutter to the right in Figure 3-1 below in the absence of **P**. If negative, the pipe will stick.

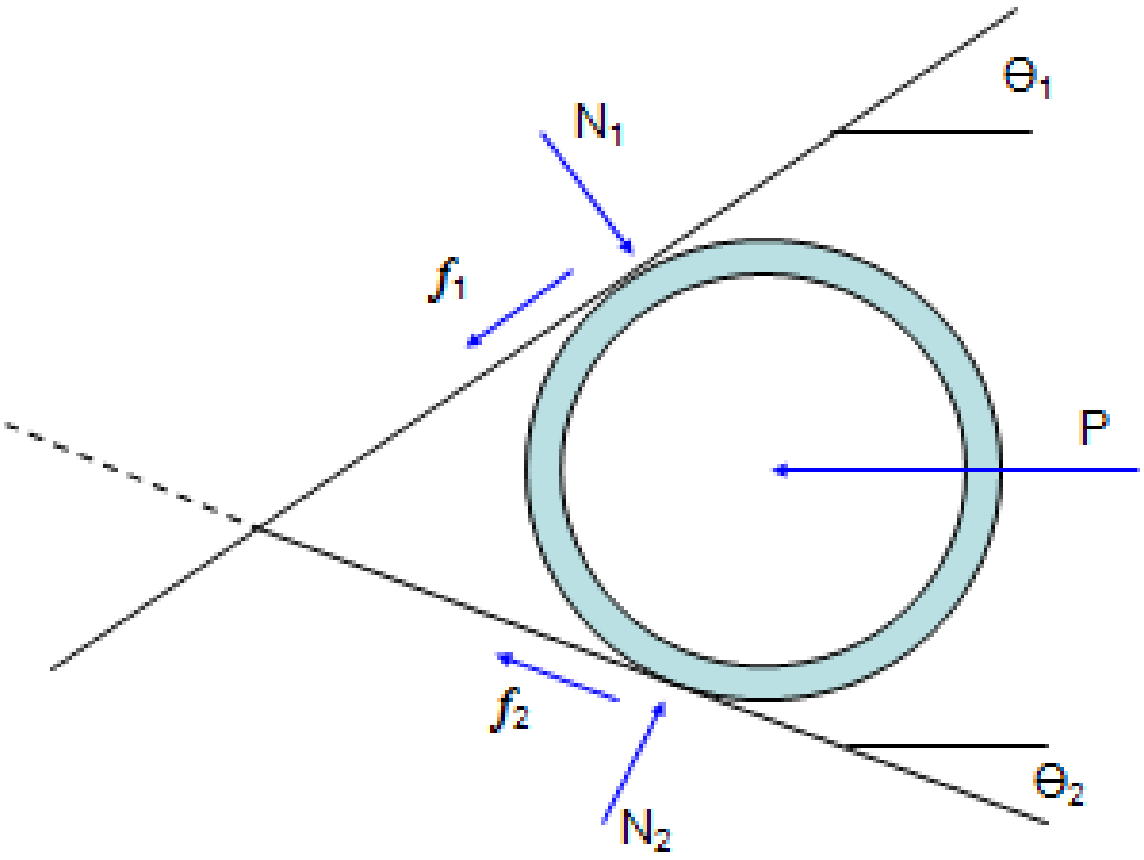

Figure 3-1. Free body diagram of general 2-blade pipe cut

At equilibrium, the sum of forces in any direction are zero, yielding equations for in-plane equilibrium:

$$N_1 \sin(\Theta_1) - f_1 \cos(\Theta_1) + N_2 \sin(\Theta_2) - f_2 \cos(\Theta_2) = P \quad [1]$$

$$N_1 \cos(\Theta_1) + f_1 \sin(\Theta_1) - N_2 \cos(\Theta_2) - f_2 \sin(\Theta_2) = 0 \quad [2]$$

$$f_1 = f_2 \quad [3]$$

Assuming Coulomb friction acting at each blade contact, at onset of sliding, at least one of the tangential friction forces has reached its upper limit:

$$f_1 = \mu N_1 \text{ or } f_2 = \mu N_2 \quad [4]$$

where **μ** is the Coulomb static friction coefficient. The other friction force would equal the one reaching its limit, and that point would not yet be sliding, but that is not required to move the pipe, because it can roll on one blade.

Single V Shear Ram

Now we assume $\Theta_1 = \Theta$ and $\Theta_2 = 0$. In this case, N_2 is also the net force from that jaw's piston, call it **F**, in other words the closing force of the ram. If the opposite side ram provides the same force **F** (or by equation [2] simplified), then:

$$N_1 \cos(\Theta) + f_1 \sin(\Theta) = F \qquad [5]$$

If we assume that f_1 has reached sliding level, we can show that for sliding conditions of $P>0$, f_2/N_2 would be greater than the friction coefficient **μ** , which is not possible for simple Coulomb static friction, so we must have f_2 reaching it's sliding level instead. Then solving equations 1 through 5, we get:

$$P = F\,[\sin(\Theta) - \mu\,(1+\cos(\Theta))(\cos(\Theta)+ \mu \sin(\Theta))] \,/\, [\cos(\Theta) + \mu \sin(\Theta)] \qquad [6]$$

Double V Shear Ram

Now we assume $\Theta_1 = \Theta_2 = \Theta$. In this case, $N_1 = N_2$ and equation 5 still holds.

If we assume that both f_1 and f_2 have reached sliding level, then solving equations 1 through 5, we get:

$$P = 2F\,[\sin(\Theta) - \mu\cos(\Theta)] \,/\, [\cos(\Theta) + \mu \sin(\Theta)] \qquad [7]$$

These equations for **P** are plotted in Figure 10 of the report for Θ = 10 degrees, and variable **μ**. Figure 10.

The spreadsheet for performing these calculations and making the plot are provided with the report cites.

ATTACHMENT 4. Testimony-Update of Dr. Rory R. Davis, PE in last 4 years

EiLand vs. Simpson Strong-Tie Co., et al
Earthquake restraint systems, patent infringement, facts witness only (inventor) for plaintiff
Deposition testimony: July, 2011
No trial yet, case in US District Court, Eastern District of Texas, Marshall Division

Bohanon v. UniSys, et al
Automated sensing equipment, outdoor protective box failure, engineer expert representing plaintiff
Deposition testimony: Oct, 2011
No trial yet, case in Sacramento, CA

ATTACHMENT 5. Testimony-Update of Patrick R. Novak, PE in last 4 years

None.

ATTACHMENT 6. Testimony-Update of J. Neil Robinson, PhD in last 4 years

None.

ATTACHMENT 7. Testimony-Update of Raymond Merala, MS, PE in last 4 years

10-22-2011	Bruno Farms v ShredAll	Depo	Superior Court, CA, Stanislaus Co.
9-23-2011	Clark v Lund	Depo	Superior Court, CA, Placer Co.
9-11-2009	Pierce v Martineau	Depo	Superior Court, CA, San Mateo Co.

ATTACHMENT 8:
LIST OF CONSIDERED MATERIALS
SINCE ORIGINAL REPORT

	Deposition Transcript & Exhibits of Ed Gaude
	All PSC Expert Reports
	All Defense Expert Reports
	Zatarain Expert Report cited materials (BP)
	Deposition Exhibit 5492
TRN-MDL-02488240 - 268	Macondo Well Integrity Test Procedures (2200-T2-DO-PR-4464)
TRN-INV-02509564 - 67	Exhibit 5661: TOI-DWH-9N9L27N-PS version 01 - AMF Sequence Test for SEM A&B
TRN-INV-02546919 - 39	Email re SEM Test Reports
	Deposition Transcript of Florence (pgs. 173 - 184 only)
	O'Donnell expert report considered materials (Cameron)
	Knight-Hawk expert report considered materials (Cameron)
TRN-INV-01130032 – TRN-INV-01130041	SEM Testing at WEST DEC, November 3, 2010
BP-HZN-2179MDL00161053-1067	Application for Bypass
TRN-INV-01465119-5618	Cameron EB702 D, Rev B9, Shearing Capabilities of Cameron Shear Rams
BP-HZN-MBI001143354-	Cameron EB 702 D, Rev B10, Shearing Capabilities of Cameron Shear Rams
TRN-INV-01653592 54091-	Cameron EB 702D RevB10 Shearing Capabilities of Cameron Shear Rams
CAM_CIV_0003105 -	Cameron Safety alert 22258
TRN-INV-00125021-032	Deepwater Horizon BOP Subsea Hydrostatic Test,
	Deposition Testimony of Fereidoun Abbassian

	Deposition Exhibits 4100-01
	Deposition Exhibit 4104
	Deposition Exhibit 215
	Deposition Exhibit 274
	Deposition Exhibit 590
	Deposition Exhibit 1159
	Deposition Exhibits 1164-65
	Deposition Exhibits 1172-73
	Deposition Exhibits 1168-69
	Deposition Exhibit 1176
	Deposition Exhibit 1183
	Deposition Exhibit 1193
	Deposition Exhibit 1199
	Deposition Exhibit 1300
	Deposition Exhibit 1356
	Deposition Exhibits 1868-70
	Deposition Exhibit 1876
	Deposition Exhibit 1878
	Deposition Exhibit 1880
	Deposition Exhibit 1890
	Deposition Exhibit 1896
	Deposition Exhibit 1300
	Deposition Exhibit 3279
	Deposition Exhibit 3276
	Deposition Exhibit 3259
	Deposition Exhibit 3175
	Deposition Exhibit 3167-68
	Deposition Exhibit 3148
	Deposition Exhibit 3298
	Deposition Exhibit 7013
	Deposition Exhibit 7008
	Deposition Exhibit 7003-4
	Deposition Exhibit 7001
	Deposition Exhibits 50166-9
	Deposition Exhibit 4423
	Deposition Exhibit 4306
	Deposition Exhibit 4112
	Deposition Exhibit 3977
	Deposition Exhibit 3976
	Deposition Exhibit 3954

	Deposition Exhibit 3948
	Deposition Exhibit 3797-98
	Deposition Exhibit 3795
	Deposition Exhibit 3605
	Deposition Exhibit 3335
	Deposition Exhibit 3343
	Deposition Exhibit 3602
	Deposition Exhibit 3952
	Deposition Exhibit 50145
	Deposition Exhibit 50162
	Deposition Exhibit 50166
	Deposition Exhibit 7025
	Deposition Exhibit 7033
TRN-INV-01827692	Investigation Ticket – Dl
TRN-INV-01841838-9	Letter from Nick Wetzel, US Department of the Interior to BP, June 25, 2008
TRN-INV-01827692	email re Operations report June 3, 2010
TRN-MDL-02971994 - 97	RMS printout
TRN-MDL-02971987-92	Daily Report 8/5/11 - Deepwater Enterprise WEST Job #3936
TRN-INV-02505078-	Design File for Calculation of Lithium MN02 Battery Life Hours and Recommended Battery Replacement, DF-055061-01
TRN-INV02505071-3	RigLORE, Engineering Report #2768
	J.C. Cunha, Buckling of Tubulars Inside Wellbores: A Review on Recent Theoritical and Experimental Works, March 2004, SPE Drilling and Completion. http://www.onepetro.org/mslib/servlet/onepetropreview?id=00087895&soc=SPE
	Deposition Exhibit 5169
	Deposition Exhibit 3130

	Deposition Exhibit 4794
	Deposition Exhibit 5297
	http://hypertextbook.com/facts/2005/steel.shtml
	http://www.engineershandbook.com/Tables/frictioncoefficients.htm
	http://www.engineershandbook.com/Tables/frictioncoefficients.htm